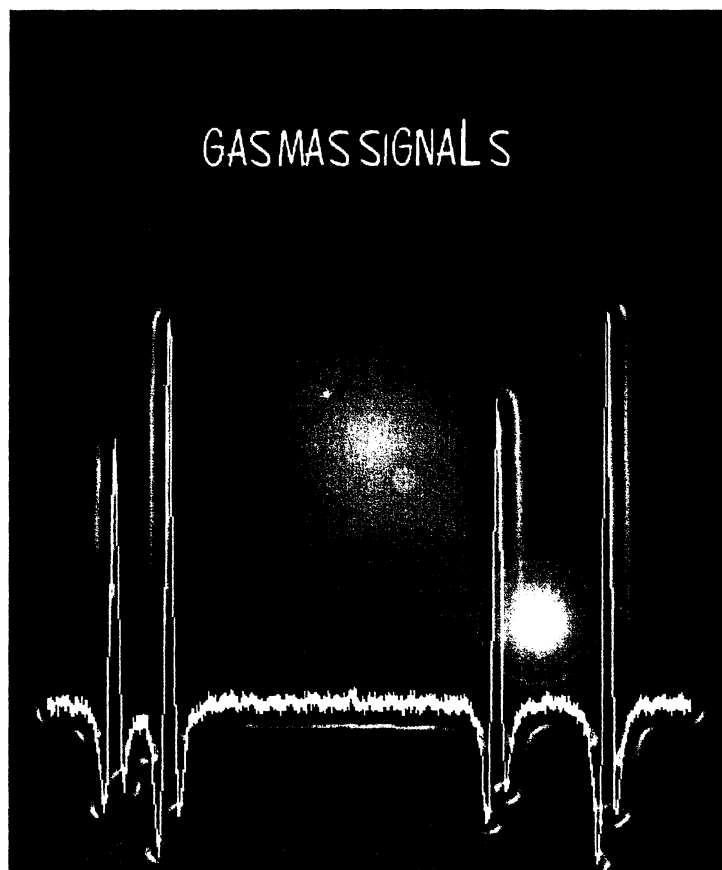


# Controlling Diode Lasers with Application to GASMAS

Master's Thesis  
by  
Billy Kaldvee

Lund Reports on Atomic Physics, LRAP-316  
Department of Physics, Lund Institute of Technology  
Lund, December 2003



## **Abstract**

In this work, GASMAS, a method for monitoring of free gas embedded in a scattering medium, has been investigated (GASMAS = GAs in Scattering Media Absorption Spectroscopy). A software package has been implemented in LabView to control a laser driver and to simplify the measurements. One subprogram measures the output power of the laser diode as a function of temperature and current. These measurements can be used by another subprogram that searches for absorption wavelengths in the wavelength span within the allowed output power. A brief theoretical and practical overview of Stark effect measurements with GASMAS is given, as a guideline for further research. Measurements have been made to find out the equivalent mean path length on apple. The temperature control in the laser holder has been studied. Two laser diodes have been characterized with the output power as a function of temperature and current. One laser has been searched through for absorption wavelengths in oxygen. Diffusion experiments have been carried out on a drying sponge, showing that the GASMAS signal from oxygen increases as the sponge gets dry.

# Table of Contents

<b>1 Introduction</b> .....	1
<b>2 GASMAS (GAs in Scattering Media Absorption Spectroscopy)</b> .....	2
2.1 The diode laser .....	3
2.1.1 Principle of operation .....	3
2.1.2 Tuning the wavelength .....	4
2.2 Absorption spectroscopy .....	6
2.3 Wavelength modulation spectroscopy .....	7
2.3.1 The lock-in amplifier .....	7
2.3.2 Frequency modulation .....	8
2.4 GASMAS, Theory and experimental setup .....	10
2.4.1 Existing experimental setup .....	10
2.4.2 Measurement techniques .....	11
<b>3 Stark effect measurement with the GASMAS method</b> .....	14
3.1 Stark Effect .....	14
3.2 Setup and methods for Stark shift measurement .....	15
<b>4 Controlling the laser measurements with GPIB (General Purpose Interface Bus) interface and DAQ (Data AcQuisition)</b> .....	16
4.1 Controlling the laser driver .....	17
4.2 Making a diagram over laser power as a function of temperature and current .....	20
4.3 Searching for absorption wavelengths .....	22
4.4 Multiple DAQ input signals .....	24
4.5 Implementation of LabView programs .....	25
4.5.1 Main program – driver control .....	25
4.5.2 Save driver setting and load driver settings .....	25
4.5.3 Control panel and power meter .....	26
4.5.4 Effect 3D graph .....	27
4.5.5 Searching for absorption wavelengths .....	28
<b>5 Experimental parts</b> .....	30
5.1 Measurements on Apple .....	30
5.1.1 Apple – thickness 4.0 cm .....	30
5.1.2 Apple – thickness 2.0 cm .....	32
5.2 Diffusion measurement on sponge .....	36
5.3 Measuring the behavior when the temperature is regulated from the laser driver .....	38
5.4 Measuring power as function of temperature and current .....	41
5.4.1 Sharp LT030MDO KAI10 .....	41
5.4.2 Sharp LT030MDO FA149 .....	42
5.5 Searching for absorption wavelengths with the LabView software .....	44
5.5.1 Current 49.8 mA .....	44
5.5.2 Current 47.0 mA .....	46
5.5.3 Current 45.0 mA .....	48
<b>6 Conclusions and summary</b> .....	49
<b>7 Future work</b> .....	50
<b>8 Acknowledgements</b> .....	51
<b>9 References</b> .....	52

# 1. Introduction

This project has been performed as a thesis for the degree of Master of Science. It has been carried out in the molecular spectroscopy group at the Atomic Physics Division of the Lund Institute of Technology.

The purpose of this project was first to get familiar with the GASMAS (GAs in Scattering Media Absorption Spectroscopy) method, then to find, develop and try different applications of it and to develop tools to make an existing and a GASMAS equipment in development easier to handle. As time went by, it showed out that there was a need for a basic software package to control the laser diode driver from the computer.

GASMAS is a method for measuring the concentration of specific gases inside a bulk material, e.g. the oxygen in the air inside a piece of polystyrene. It is based on the fact that the bulk material has a very broad absorption pattern compared to the narrow absorption peaks of, e.g., gaseous oxygen. On the other hand the absorption from oxygen can be very small in this context and it takes special methods to be able to detect this small absorption. The sensitive method used in GASMAS measurements is wavelength modulation spectroscopy.

During the project a software package has been developed to control the laser driver and to collect data from photo diodes and other measuring instruments. Research about different applications now possible and regarding applications, which will become possible in a near future, has been done. Some of those applications are described in this thesis and others fall outside the scope of this master's thesis.

In Chap. 2 it is described how a laser diode works and the theory that is needed to understand how the GASMAS method works is described. In Chap. 3 one of the possible applications of GASMAS, Stark effect measurements, is described briefly. In Chap. 4 both the functionality and the field of application of the software package that has been implemented is described thoroughly. Chap. 5 contains descriptions and results of the different experiments that have been carried out. Chap. 6 summarizes the conclusions and, finally Chap. 7 gives suggestions for future research and a brief guideline to how the software package should be further developed to automate the whole GASMAS process.

## 2. GASMAS (GAs in Scattering Media Absorption Spectroscopy)

### 2.1 The diode laser

The diode laser is a semiconductor-based laser, which is very small, cheap and easy to handle compared with other types of lasers. It was first demonstrated in 1962 [2.1-2.4], but the development was very intense during the 1980's, when the diode laser changed from being a device used in a laboratory environment to a device used in home electronics such as CD players. The wavelength range of diode lasers is from 390 nm to 30  $\mu\text{m}$  [2.5]. Something that limits spectroscopic measurements, e.g. with GASMAS, is that there are only diode lasers commercially available in some regions of this range. The most common types of semiconductor lasers, e.g. the widely used GaAs lasers, are based on combination of elements from the third and fifth group of the periodic system. The wavelength from these lasers ranges from 630-1600 nm [2.6]. For a better overview of the principles of laser the reader is referred to [2.6].

#### 2.1.1 Principle of operation.

Fig. 2.1 shows a semiconductor in two different states. In Fig. 2.1 (a) all electrons in the semiconductor are in the valence band V and the conduction band C is empty. These bands are equivalent to different electron energies. The band structure is a schematic picture where the energy distribution of all the electrons in the actual area can be seen.

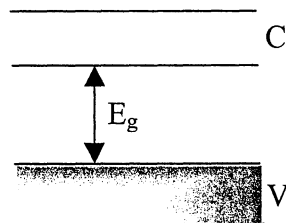


**Fig. 2.1 (a)** Valence and conduction band in a semiconductor

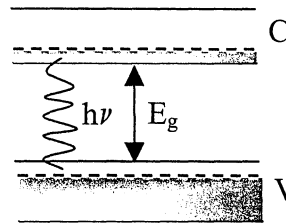


**Fig. 2.1 (b)** Valence and conduction band with electrons in the conduction band

If we start filling the conduction band with electrons and remove electrons from the valence band, by some proper pump process, the band structure will look like in Fig. 2.1 (b). When there are electrons in the conduction band and there is deficit of electrons in the valence band they will fall down to the valence band in a very short time. When they fall down they will send out light with the energy  $h\nu$ . This process is the one by which light is sent out in light-emitting diodes. If a correctly designed pump mechanism is used stimulated emission can be reached, which will lead to laser action.

The pumping can be achieved in different ways, e.g. by exciting the semiconductor with another laser- or electron beam. But the most common and convenient way to pump a semiconductor laser is to use it as a diode. The current flowing in the forward direction of the junction then serves as the pump mechanism [2.6]. For the full physics of semiconductor devices the reader is referred to [2.7]. In Fig. 2.1 (c) the band structure of a p-n junction with p-type and n-type of the same semiconductor material is shown. This is called a homojunction laser. In this first case there is no voltage applied. On the p-side there is an excess of holes,

also called acceptors, which means a deficit of electrons in the valence band. And on the n-side there is an excess of donors, electrons, in the conduction band. It is readily understood that if you put a n-type semiconductor together with an p-type semiconductor, electrons would like to fall from the conduction band on the n-side to the valence band on the p-side to recombine. But when no voltage is applied, the energy structures for the two sides are configured in a way that cannot let the electrons and holes recombine. In Fig. 2.1 (d) it is shown what happens with the band structure when a forward-bias voltage is applied. Electrons are injected in the active region from the conduction band on the n-side and holes are injected from the p-side. This allows them to recombine in a small area called the active region. For sufficient values of the current density, i.e. the forward-bias voltage, the laser threshold condition can be reached.

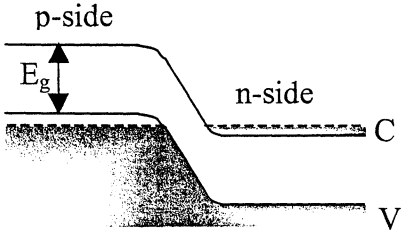


Fig. 2.1 (c) Band structure of p-n junction without any voltage

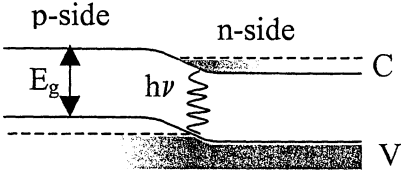


Fig. 2.1 (d) Band structure of p-n junction with forward-bias voltage

The type of semiconductor laser in common use and the one that we use in GASMAS is the Double-Heterostructure Laser, which basically looks as in Fig. 2.2 (a). There are many advantages with this type of structure. The most striking one is that laser action can occur at room temperature. The reason why it is possible to operate at room temperature is due to the way an active layer is put in between two layers of p-type and n-type.

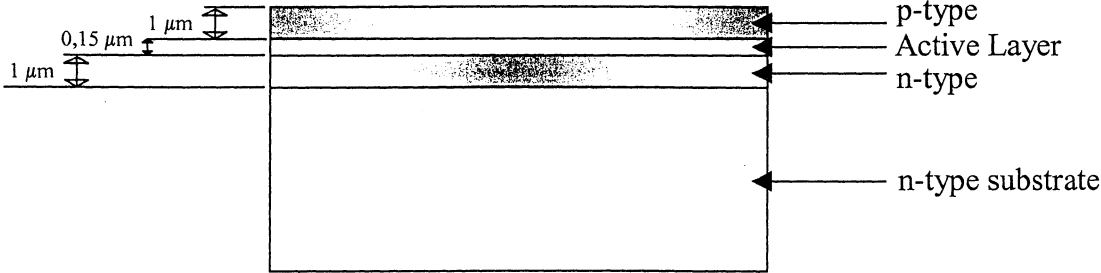
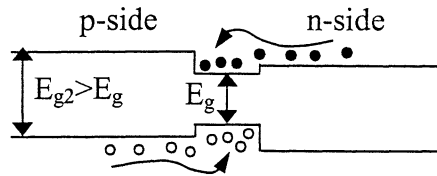


Fig. 2.2 (a) Heterostructure semiconductor Laser

The active layer has a smaller bandgap and different refractive index than the p-side and n-side. The difference in refractive indices gives reflection in the surface between the layers, which guides the laser light along the active layer. The smaller bandgap helps catching in electrons and holes inside energy barriers as can be seen in Fig. 2.2 (b). This is very desirable since the electrons otherwise rush in to the p-side, and holes to the n-side, where they can recombine and make the laser ray wider. And a wider ray needs greater current to keep lasing.



**Fig. 2.2 (b)** Band Structure in Heterostructure semiconductor laser

To achieve laser action, a cavity, an optical resonator, is needed. In other types of laser this cavity is external with mirrors, but in diode lasers the medium itself can be used as a cavity. The surfaces between the active layer and the surrounding air, which are prepared by cleavage along crystal planes, serve as mirrors. The difference in refractive indices gives a reflectance of 30%. The wavelength is determined by the bandgap of the semiconductor material in the active layer. As mentioned before, laser action will not be achieved until the current is strong enough to satisfy the lasing condition. This current is called the threshold current. At currents higher than the threshold current, the output power is proportional to the current. When the temperature of the laser is changed, the semiconductor gain is changed and thus the output power and threshold current is changed as well. In Fig. 2.2 (c) the output power is shown for three different temperatures,  $T_1 < T_2 < T_3$ .

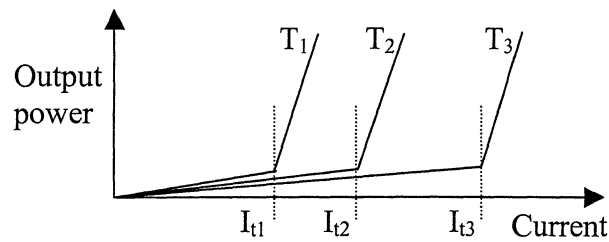


**Fig. 2.2 (c)** The output power as a function of the current for three different temperatures  $T_{1-3}$ .  $I_{th1-3}$  are the different threshold currents

### 2.1.2 Tuning the wavelength

The wavelength of a diode laser is tuned by changing the temperature of the laser. The change in wavelength is due to a temperature dependence of the bandgap and a temperature dependence of the refractive index, which changes the path length and thereby the wavelength. The largest effect is due to the temperature dependence of the bandgap, which changes the wavelength by about  $0.25 \text{ nm}/^\circ\text{C}$  [2.5]. The temperature can be changed by the use of a Peltier element or by varying the current. The Peltier element is mostly used for coarse-tuning and the current is then used for fine-tuning. The temperature dependence of the wavelength will typically look as in Fig. 2.3

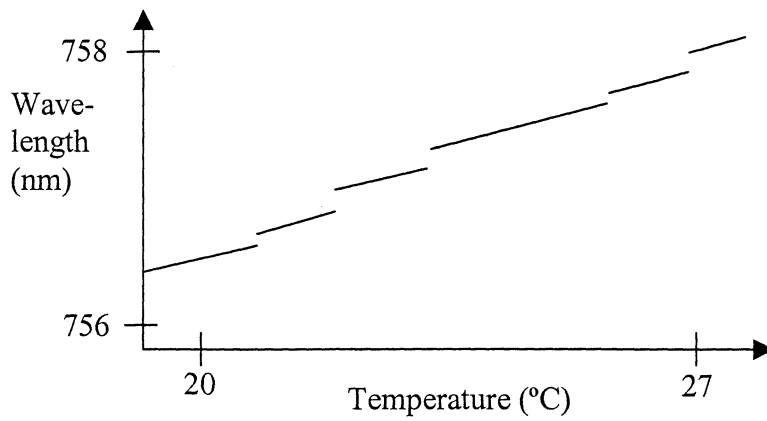


**Fig. 2.3** Temperature dependence of wavelength in a semiconductor laser

A common way to modulate the wavelength is to superimpose a saw-tooth formed current over the operating current. That gives a possibility to do fast wavelength sweeps over small wavelength regions. When a sinus waveform with higher frequency is superimposed over the saw-tooth waveform, frequency modulation spectroscopy can be performed [2.5].

## 2.2 Absorption spectroscopy

Absorption spectroscopy is an essential element of the GASMAS method. It is normally used in specific volumes of gas, which can be an enclosed sample or out in free air. The absorption of light in gas is governed by Beer-Lambert's law, where the measured intensity  $I(\nu)$  is related to the original intensity  $I_0(\nu)$  as

$$I(\nu) = I_0(\nu) \exp[-\sigma(\nu)cL]. \quad (2.1)$$

$\sigma(\nu)$  is the absorption cross section per molecule,  $c$  is the concentration of absorbing gas molecules and  $L$  is the absorption path length. Beer-Lambert's law is often written like

$$I(\nu) = I_0(\nu) \exp[-a(\nu)], \quad (2.2)$$

where  $a(\nu)$  is the absorbance. The intensity of light sent through an absorbing sample will decrease exponentially as illustrated in Fig. 2.4

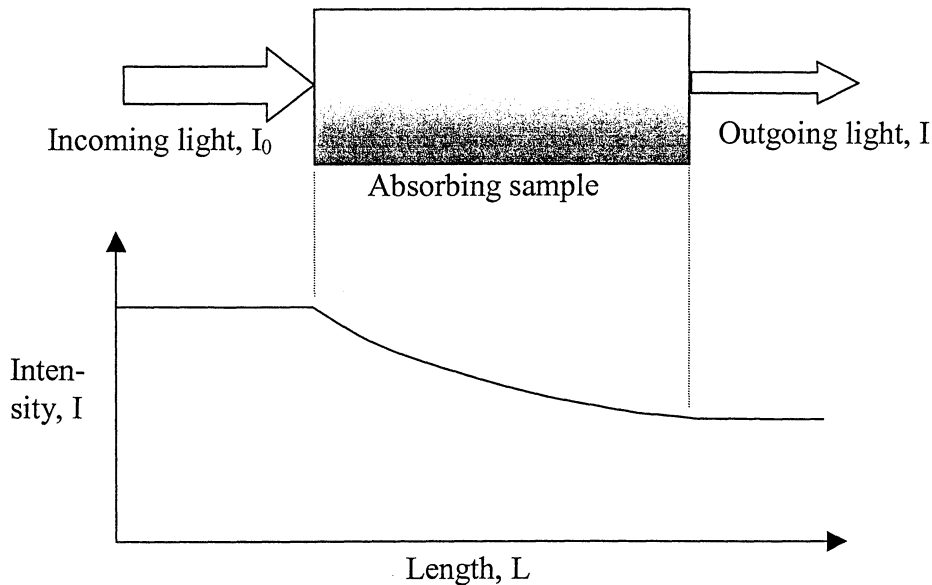


Fig. 2.4 Illustration of Beer-Lambert's Law

This is also the relation being used in GASMAS experiments. From spectroscopic measurements only  $a(\nu)$  can be calculated. Thus  $\sigma(\nu)$  and  $L$ , two of the unknown factors in  $a(\nu)$ , has to be determined by other means to calculate the concentration  $c$ .

## 2.3 Wavelength modulation spectroscopy

Wavelength modulation spectroscopy (WMS) [2.8] is one of three common frequency modulation techniques [2.5]. The other two are frequency modulation (FM) and two-tone frequency modulation spectroscopy (TTFMS). There is also a method called amplitude modulation. All of those methods are used to get a better signal-to-noise ratio by reducing the noise. In the GASMAS experiments we are using WMS. The setup for WMS is shown in Fig. 2.5.

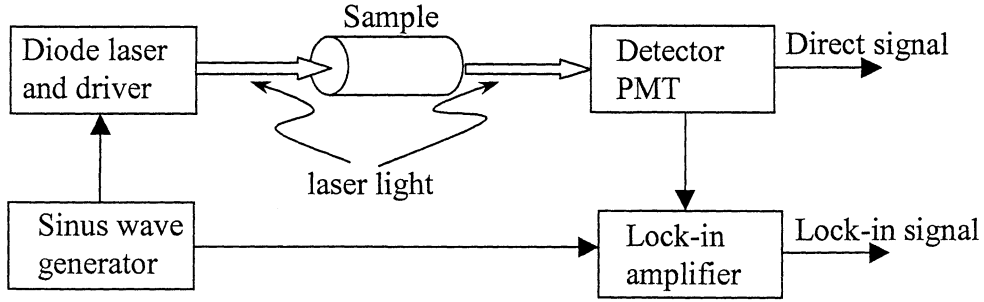


Fig. 2.5 Setup for wavelength modulation spectroscopy

When doing WMS in GASMAS experiments a sinus wave generator is used to superimpose a current to the laser driver with a frequency,  $\nu_m$ , around 50 kHz, which is small compared to the linewidth of the absorption signal, which is in the GHz range. The sinus wave is at the same time sent to a lock-in amplifier as a reference signal. The output from the lock-in amplifier, the lock-in signal, resembles the first derivative of the direct signal. Instead of looking at  $\nu_m$  the lock-in amplifier can use the double frequency  $2 \cdot \nu_m$ , which is done in the GASMAS measurements. Then the lock-in signal will resemble the second derivative of the direct signal. It has been shown that frequency modulation techniques can record absorption down to the shot-noise limit, which practically means that absorption detection down to one part in  $10^6$  is possible [2.9].

### 2.3.1 The lock-in amplifier

It can be shown why the lock-in signal resembles the derivative of the direct signal. Fig. 2.6 shows an absorption spectrum where two different wavelengths,  $\lambda_1$  and  $\lambda_2$ , are treated in detail. A superimposed current, with frequency  $\nu_m$ , gives a modulation,  $\Delta\lambda$ , to the laser wavelength,  $\lambda$ . The lock-in input signal at  $\lambda_1$  will be an ac signal with amplitude,  $S$ , and an offset  $A$ . At  $\lambda_2$  it will be a dc signal with an offset  $B$ . The lock-in input signal is amplified by an ac-amplifier, which contains a bandpass filter centered at the modulation frequency,  $\nu_m$ . Then it is multiplied in a multiplier circuit with an internal reference signal,  $V_0(t)$ , which has been created with the same frequency,  $\nu_m$ , as the external, sinusoidal, reference modulation signal. If  $V_0(t)$  is sinus shaped we get [2.10]

$$\begin{aligned}
 V_{mix}(t) &= V_0(t) \cdot V_{ac}(t) = E_0 S \cos(2\pi\nu_m t) \cdot \cos(2\pi\nu_m t + \theta) = \\
 &= \frac{1}{2} E_0 S [\cos(\theta) + \cos(4\pi\nu_m t + \theta)]
 \end{aligned} \tag{2.3}$$

where  $V_{ac}(t)$  is the lock-in input signal component containing the reference frequency,  $\nu_m$ , and  $\theta$  is the unknown phase difference between the reference signal and the lock-in input signal.

Notice that all ac components with frequencies apart from  $\nu_m$  will produce time dependent contributions without dc components. This can be seen from the last two cosine terms in Eq. 2.3. They are a result of the trigonometric relationship:  
 $\cos(\alpha) \cdot \cos(\beta) = \frac{1}{2}(\cos(\alpha - \beta) + \cos(\alpha + \beta))$ . The output signal  $V_{out}$  is produced by letting  $V_{mix}$  pass through a low pass filter and the only dc component is

$$V_{out} = \frac{1}{2} E_0 S \cos(\theta), \quad (2.4)$$

which is directly proportional to the amplitude,  $S$ , of the lock-in input signal. From Fig. 2.6 it can be seen that the amplitude  $S$  is measuring the derivative in the current point. It is obvious that the phase difference,  $\theta$ , should be adjusted to 0 by a built in phase-shifting circuit to record a strong signal, proportional to the derivative of the lock-in input signal.

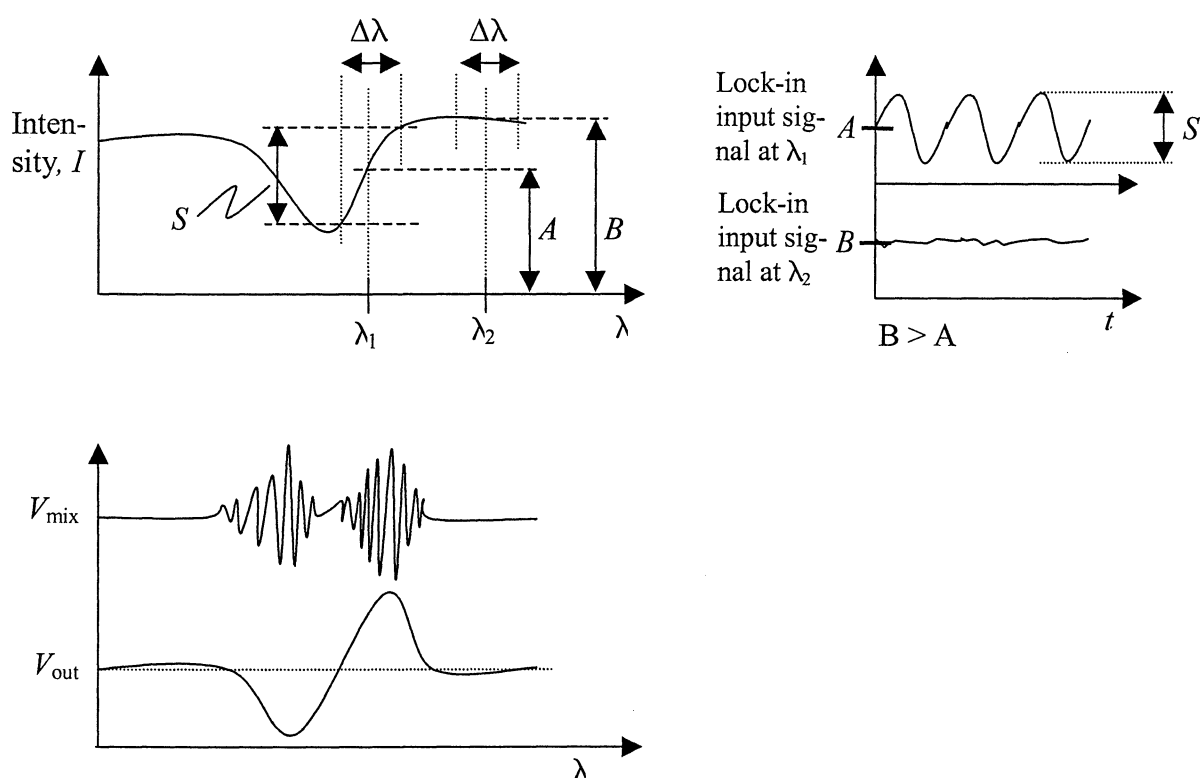
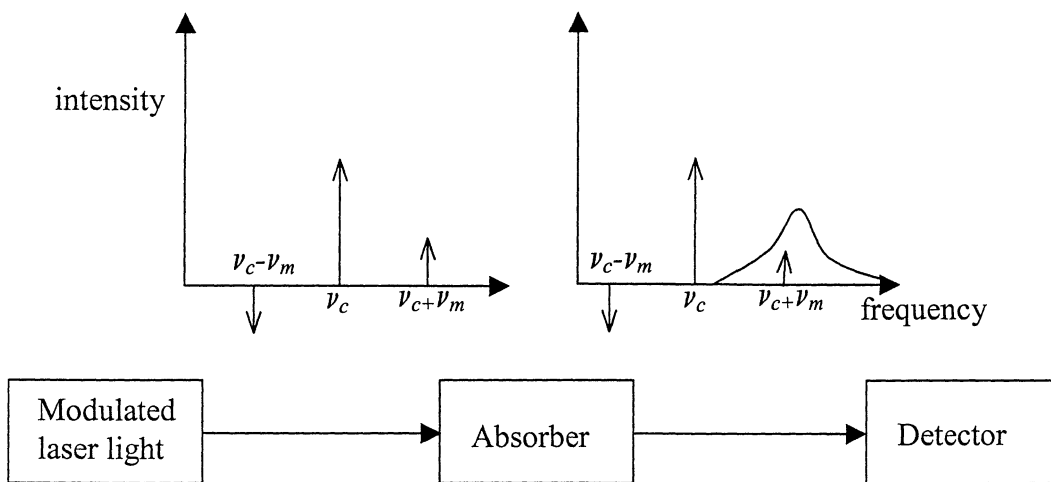


Fig. 2.6 Illustration of the lock-in technique in wavelength modulation spectroscopy

### 2.3.2 Frequency modulation

If the modulation frequency gets considerable higher, into the MHz-GHz range, another approach is used to explain how the method works. The modulation of the laser driver leads to the generation of sidebands, which can be seen in Fig. 2.7, where  $\nu_c$  is the laser frequency and  $\nu_m$  is the modulation frequency. A simplified description of how the output signal is produced is that when the two sidebands are not absorbed equally much a beat signal will be produced. This means that the larger the difference in absorption is at the two sidebands the larger the beat signal will be. Each sideband passes over the absorption line ones while the other does not get absorbed. This leads to a signal that will look roughly as  $V_{out}$  in Fig. 2.6, which is similar to the derivative of the absorption pattern that is seen in the direct signal.



**Fig. 2.7** Generation of sidebands and what happens when the wavelength modulated light passes through absorbing material [2.5].

## 2.4 GASMAS, Theory and experimental setup

GASMAS is a method for monitoring of free gas embedded in a scattering medium. Examples of materials where the method has been applied are fruit, wood and polystyrene foam [2.11]. The method is easy to use and opens up many possibilities for future research.

### 2.4.1 Existing experimental setup

The setup consists of three important parts: the diode laser system, the scattering medium and a photo multiplier followed by detection electronics. An existing setup looks as in Fig. 2.8.

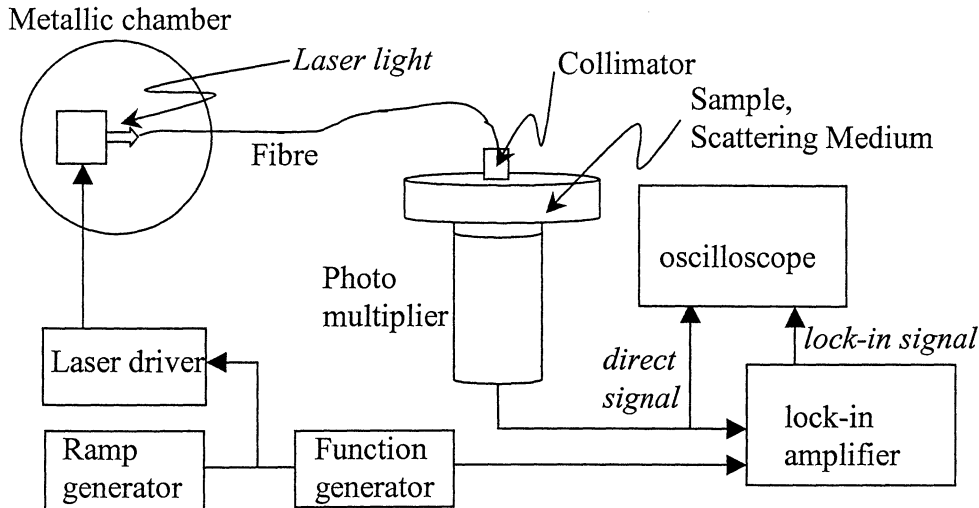


Fig. 2.8 The existing GASMAS setup [2.11]

So far a single-mode diode laser (Sharp LT031MDO) with a nominal wavelength of 757 nm at 25°C has been used to monitor an oxygen line (R7R7) at 761.003 nm in the oxygen A band. The laser sweeps over the wavelength 761.003 nm when superimposing a saw-tooth signal from the ramp generator with an amplitude of 600 mV and a period of 250 ms. The laser is operated in a thermoelectrically cooled holder, which is controlled by a diode laser driver, which is set to a temperature of 46°C and a current of 57.2 mA. The laser is placed together with a lens that focuses the light into a 600  $\mu\text{m}$  quartz fibre. A fibre is used to get rid of the unwanted oxygen absorption that is present in air. Both the metallic chamber and the collimator is nitrogen flushed for the same reason, to get rid of unwanted oxygen absorption. By taking this precautions we can be sure of getting unaffected laser light out of the collimator. When the light has passed through the sample it is normally very weak. To collect it a sensitive detector, a photomultiplier tube (EMI 9558 QA) is used. It is protected from the ambient light by a coloured glass filter that cuts off at wavelengths lower than 695 nm. Theoretically the direct signal from the photomultiplier will look as in Fig. 2.9.

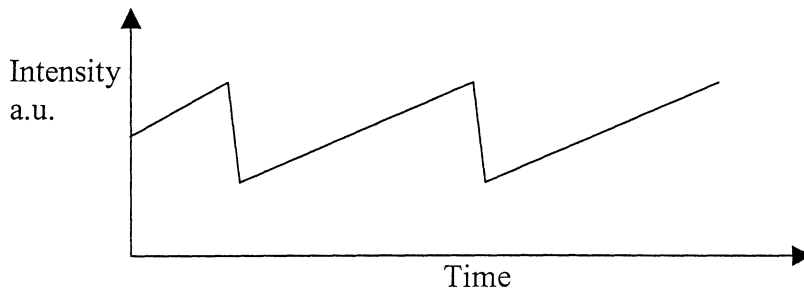


Fig. 2.9 Theoretical direct signal from the photomultiplier

We now want to observe the absorption caused by oxygen. As seen in Fig. 2.9 it cannot be seen in the direct signal most of the times, because the absorption is very small, which makes the signal small and the signal-to-noise ratio small. The way to make it visible is by using frequency modulation as mentioned in Chap. 2.3. It is used with a frequency of 55 kHz. The lock-in amplifier uses the double frequency to produce its signal, which will look as the second derivative [2.12]. If the direct signal and the lock-in signal are displayed at the same time it will schematically appear as in Fig. 2.10.

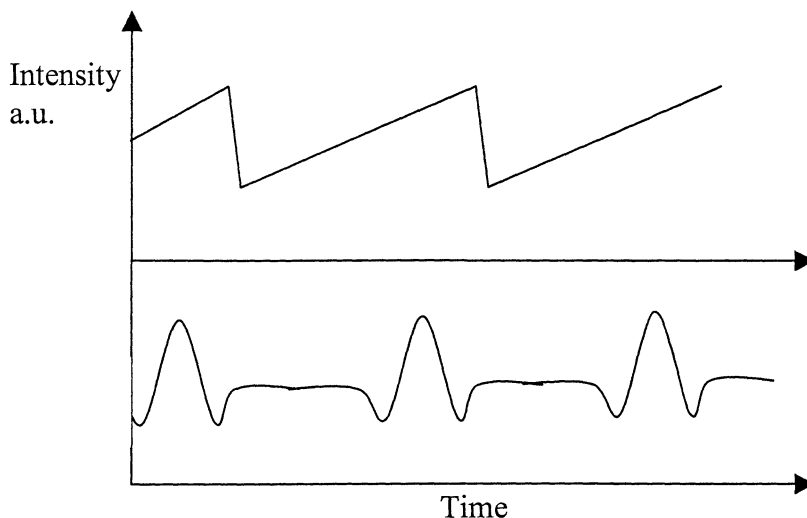


Fig. 2.10 Theoretical direct- and lock in signal

### 2.4.2 Measurement techniques

To compensate for variations in the detected light intensity a quotient between the lock-in signal and an interpolated direct signal is used. In this way, a normalized signal,  $S_{norm}$ , is achieved [2.13]. For definitions, see Fig. 2.11 (a). Interpolated signal means that if there is a small absorption visible in the direct signal, it is neglected when measuring  $S_{ref}$ , which can be seen in Fig. 2.11 (b).

$$S_{norm} = \frac{S_{lock}}{S_{ref}} \quad (2.5)$$

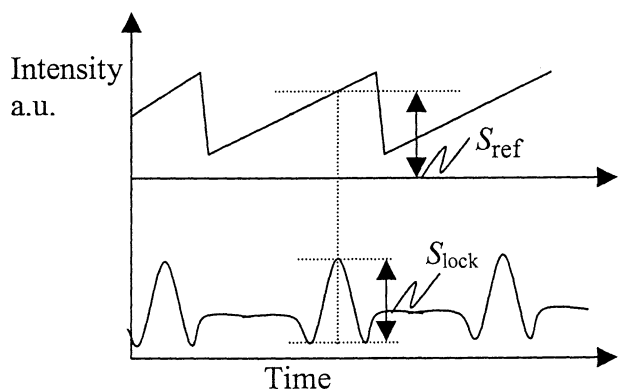


Fig. 2.11 (a) Definition of  $S_{lock}$  and  $S_{ref}$

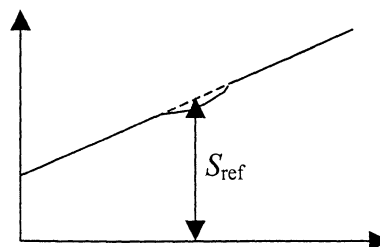


Fig. 2.11 (b) How to interpolate the direct signal

By the use of the well-known standard addition method, it is possible to calculate an equivalent mean path length,  $L_{eq}$ . In this case equivalent mean path length means how long the laser light would have to go through normal air to get the same absorption as in the scattering medium. The method is based on the principle of adding a known amount of air and then in our case, by using a linear relationship between  $S_{norm}$  and the path length,  $L_{eq}$ , we can calculate  $L_{eq}$  for small real path lengths. This is illustrated in Fig. 2.12. The linear relationship between  $S_{norm}$  and  $L_{eq}$  can be seen theoretically from Eq. 2.1, where  $e^{-x} \approx 1 - x$  for small  $x$ .

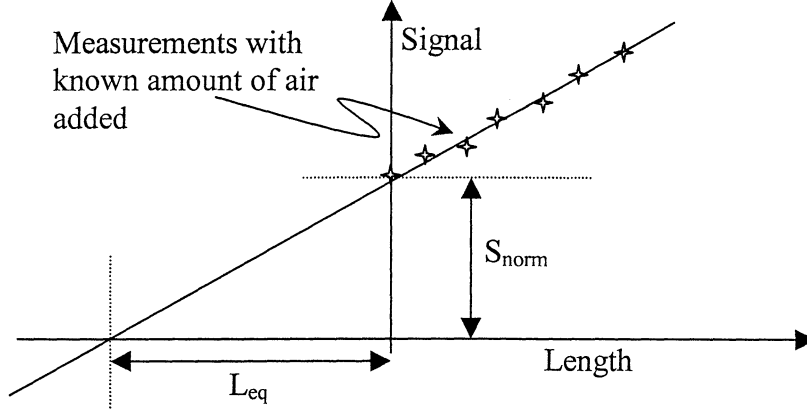


Fig. 2.12 Illustration of the standard addition method

One quantity that is interesting to measure is the concentration,  $c_{sm}$ , of the current gas concentration, i.e. oxygen, within the scattering medium. From Eq. 2.1 we can set up one expression for the equivalent path length and one for the real path length in the scattering medium

$$I(\nu) = I_0(\nu) \exp[-\sigma(\nu)c_{sm}L_{sm}] = I_0(\nu) \exp[-\sigma(\nu)c_{air}L_{eq}], \quad (2.6)$$

where  $c_{air}$  is the concentration of oxygen in air. Eq. 2.6 leads to

$$\sigma(\nu)c_{sm}L_{sm} = \sigma(\nu)c_{air}L_{eq} \Rightarrow c_{sm} = c_{air} \frac{L_{eq}}{L_{sm}}, \quad (2.7)$$

where  $L_{sm}$  is the only unknown since  $c_{air}$  is an easily obtained constant.

We find that the determination of  $L_{sm}$  is the hardest part. It is very thoroughly described in [2.12, 2.13]. So far another setup has been used to do this, a time resolved spectroscopy setup [2.14], but  $L_{sm}$  can also be calculated with the use of a transport model for light propagation within the sample. From time resolved spectroscopy the mean time of flight,  $\langle t \rangle$ , is determined and then  $L_{sm}$  is calculated as follows.

$$L_{sm} = \frac{c_0}{n_{sm}} \langle t \rangle \quad (2.8)$$

$\langle t \rangle$  is the mean time of flight, i.e. the average time spent by photons in the scattering medium,  $n_{sm}$  is the refractive index of the scattering medium and  $c_0$  is the speed of light. The refractive index can be estimated as a combination of the refractive index of the bulk material and the refractive index of the gas, as shown in Eq. 2.9, when the scattering medium is

homogeneous and isotropic according to [2.13]

$$n_{sm} = Pn_{air} + (1 - P)n_b, \quad (2.9)$$

where  $P$  is the porosity of the material and  $n_b$  is the refractive index of the bulk material. According to [2.12] the porosity of material with substantial gas diffusion and without internal sources/sinks, i.e. in equilibrium with the surrounding can be written

$$P = \frac{c_{sm}}{c_{air}} \quad (2.10)$$

Using Eqs. 2.7-2.10,  $c_{sm}$  can be evaluated from the equation

$$c_{sm} = \frac{c_{air}L_{eq}}{c_0 \langle t \rangle} \left( \frac{c_{sm}}{c_{air}} n_{air} + \left[ 1 - \frac{c_{sm}}{c_{air}} \right] n_b \right) \quad (2.11)$$

### 3. Stark effect measurement with the GASMAS method

The Molecular Spectroscopy Group are planning to do GASMAS measurements on scattering media, such as porcelain insulators, exposed to an electric field. The shape of the GASMAS signal will carry information on the fraction of time the photons have passed through volumes of different field strengths. In this way the absorption pattern of the scattering medium will be affected by the Stark effect, which is varying through the sample. The GASMAS signal may provide an indirect way to measure the electric field inside the material. Alternatively, for a well-known electric field distribution, information on the gas distribution might be achieved through tomography. Electric fields in air mixtures surrounding electrical components have been measured by laser spectroscopy on  $\text{NH}_3$  by Höjer et al. [3.1].

#### 3.1 The Stark effect

The Stark effect may be observed as changes in the absorption spectrum of a gas under the influence of an electric field. The changes arise from the torque that the electric field exerts on the molecular electrical dipole moment. This torque changes the rotational motion and thus the rotational spectrum of the molecule. The new energies,  $W$ , of the rotational states in the system is given by

$$W = W_0 - \bar{\mu}_E E, \quad (3.1)$$

where  $\mu_E$  is the mean component of the electrical moment in the field direction [3.2] and  $W_0$  is the undisturbed energy levels. The Stark effect gives both an offset in the energy level and splits it up into more levels, which can be understood if  $\mu_E$  is examined closer. If a molecule is in its electronic ground state denoted  $\Sigma$ ,  $\mu_E$  can be written as a second order approximation [3.2].

$$\bar{\mu}_E = -\frac{4\pi^2 I_0 \mu^2}{h^2} \left[ \frac{J(J+1) - 3M^2}{J(J+1)(2J-1)(2J+3)} \right] E, \quad (3.2)$$

where  $J$  is the rotational quantum number and  $M$  is the magnetic quantum number, which is defined as  $M = -J, -J+1, \dots, 0, \dots, J-1, J$ .  $I_0$  is the moment of inertia and  $\mu$  is the electric dipole moment. If the molecule is in an electronic state  $\Lambda \neq 0$ , there is also a linear effect that is a first order approximation and hence dominates the Stark effect. Then the electrical moment is written

$$\bar{\mu}_E = \frac{\mu M \Lambda}{J(J+1)}, \quad (3.3)$$

Since the electric dipole moment and the effective moment of inertia has a minor dependence on the vibrational quantum number, very small differences in the energy shift of the vibrational states can occur. Symmetrical molecules have no electric dipole moment and are thus not particularly affected by electric fields [3.3]. They are only affected by a small quadratic Stark shift. A small electric dipole moment is induced by the electrical field giving rise to a electric moment, and hence a quadratic shift.

$$\bar{\mu}_E = \alpha E \Rightarrow W = W_0 - \alpha E^2, \quad (3.4)$$

where  $\alpha$  is a constant depending on the quantum numbers  $J$  and  $|M|$ .

### 3.2 Setup and methods for Stark shift measurements

The basic setup should look as in Fig. 2.8. The only thing that should be changed is that the sample should be contained in a cell with electrodes. The cell should have a gas inlet to be able to let the GASMAS gas in. The cell should schematically look as in Fig. 3.1. Electric fields can be applied up to about 30 kV/cm without inducing electrical breakdown [3.4]. This should be kept in mind when preparing an experiment.

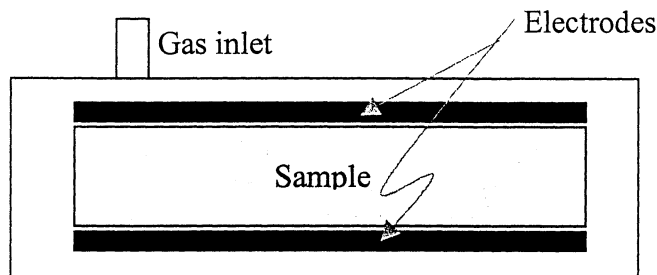


Fig. 3.1 Schematic overview of a GASMAS cell for Stark experiments

If an experiment is done in normal air pressure, the splitting of the absorption peak will not be resolved. Thus the effect will be that the absorption peak broadens and the absorption maximum moves in wavelength.

Since oxygen, the gas used in GASMAS measurements so far, is a symmetric molecule, the Stark effect is not very large according to Chap. 3.1. Hence, another molecule has to be used for Stark effect measurements. Stark shifts has been detected in  $\text{NH}_3$  by the use of semiconductor lasers at  $1.23 \mu\text{m}$  [3.4], making it a good candidate for GASMAS use. The size of the Stark shift is in the GHz range when applying an electric field of 25 kV/cm. As the peaks have a FWHM smaller or equal to this shift it is reasonable to believe that the differences in the GASMAS signal should be measurable when applying an electric field. If the Stark shift turns out to be very small it can still be detected if the laser wavelength is set to coincide with one of the edges of the absorption peak when no field is applied. Then, we will be standing on a point in the absorption pattern that has a large derivative and thus be very sensitive to electric fields when the peak moves according to the Stark shift. If the electric field is amplitude modulated and the same frequency is used in the reference signal to the lock-in amplifier it will mean that the output signal from the lock in amplifier will be strongly related to the Stark effect. In Fig. 3.2 a quantitative example of a Stark shifted absorption line at low pressure is shown. If the measurements are made at higher pressure or normal air pressure, the well resolved Stark shifted components will blur out to one asymmetric broader peak.

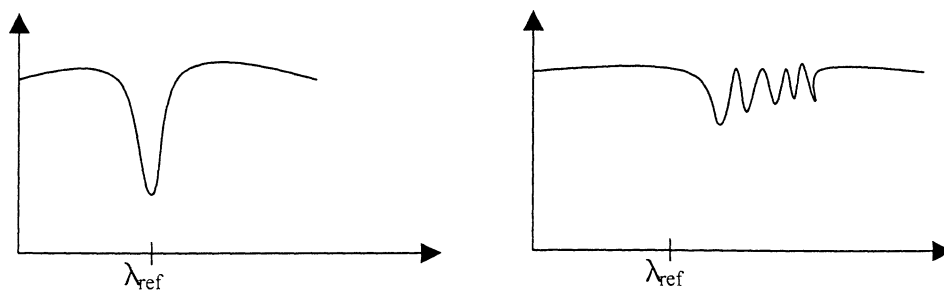


Fig. 3.2 Stark splitting of an absorption line at low pressure

## 4 Controlling the laser measurements with GPIB (General Purpose Interface Bus) interface and DAQ (Data Acquisition)

Controlling the measurements from a computer needs a lot of software if it is supposed to be user friendly. All of the software developed within the present diploma paper is made in LabView, a graphical programming language provided by National Instruments. In LabView the programs called VI:s, virtual instruments, are built up by block diagrams, which means that the source code is a diagram with different blocks connected to each other with wires when needed for data to flow properly. Besides that each program has a front panel, which is the user interface.

The main program that we have developed to control the laser driver experiments is essentially a menu to reach the subprograms that take care of different tasks. Besides that, the settings from the laser driver are read in and the most important ones are displayed on the screen. In Fig. 4.1 the main program is shown. When the main program initializes it reads in and displays the current settings from the laser driver and displays them on the screen. Then it is waiting for the user to choose one of the subprograms to run by clicking on it.

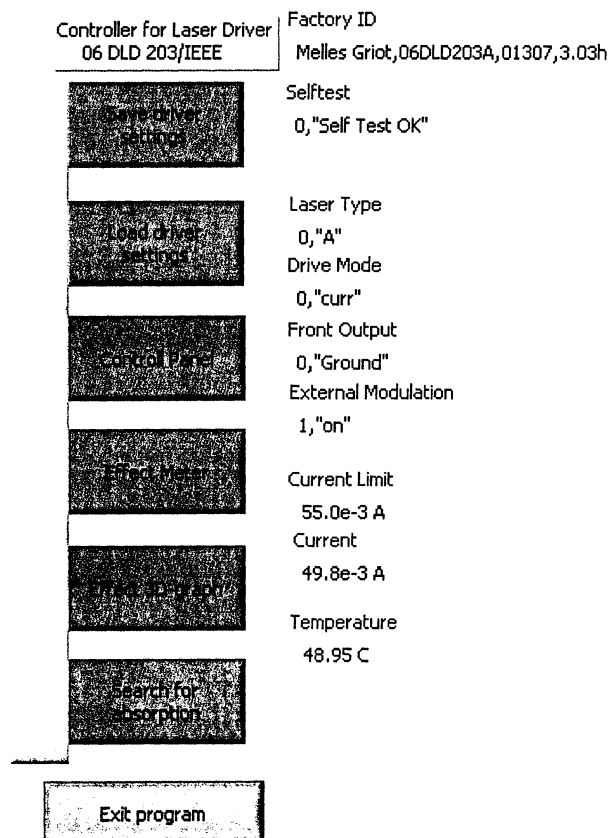


Fig. 4.1 The Main program for driver control

## 4.1 Controlling the laser driver

The laser driver, Melles Griot model 06DLD 203/IEEE, is an electric unit that controls the temperature of the laser and the forward bias current in the laser diode. As described in Chap. 2.1, these are the parameters that decide what the output wavelength of the laser will be. That is why the ability to control the laser driver was the first that had to be implemented and thoroughly understood to be able to make any further progress with computer based experimental work. The laser driver is also capable of giving us useful information, such as the temperature of the laser diode and a monitor current, from a photo diode inside the laser holder, that is proportional to the output power from the laser. All of the communication with the laser driver is accomplished via a communication protocol called GPIB (General Purpose Interface Bus). The GPIB card used in the computer is a National Instruments™, GPIB-USB-B.

The "Control panel" is used to control and overview some of the basic settings on the laser driver. A temporal overview of the temperature and current is given here as well. A picture of the interface is shown in Fig. 4.2.

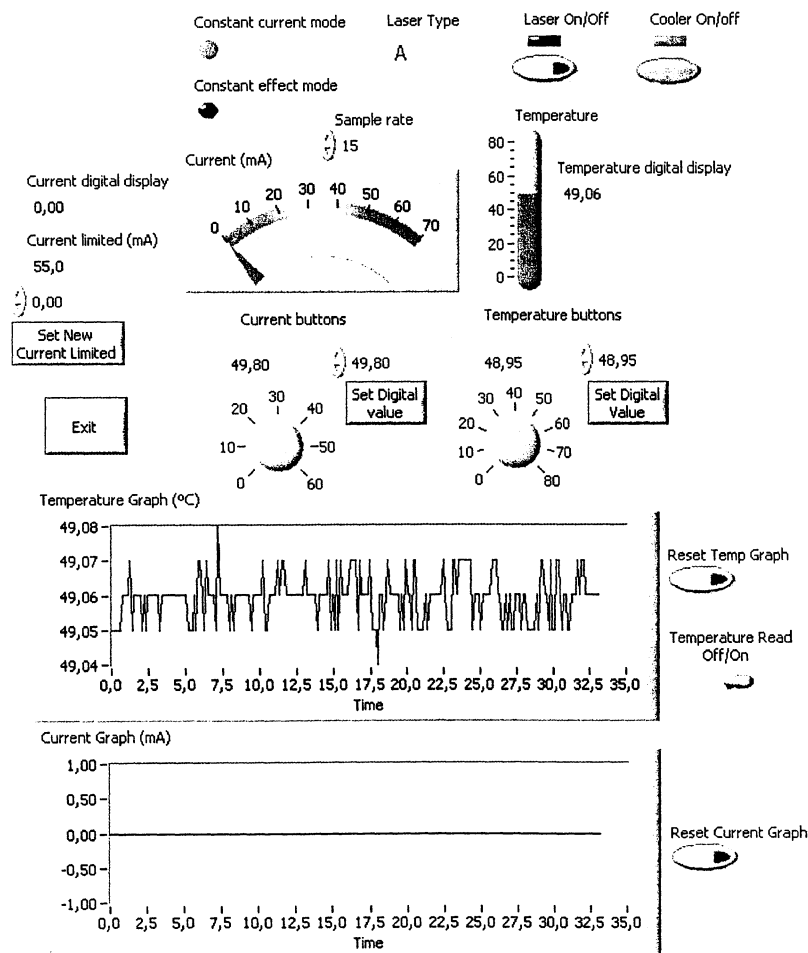


Fig. 4.2 Picture of the control panel

On top of the control panel there are three indicators that cannot be changed. It is the "Laser type" indicator that shows the user what kind of laser the driver is set to drive. This can be changed manually on the driver. The other two not changeable indicators are the "Constant

current mode” and “Constant power mode”. They show in which one of those two modes the laser driver is set. The “Sample rate” control is used to set the rate that the software will try to acquire all information from the laser driver. This is limited by the laser driver, which cannot answer more than 12-16 questions per second via the GPIB port. Since the control panel shows both the temperature and current, the maximum sample rate is 6-8 Hz. Both the current and the temperature are shown at three different places each, in the live analog meters with accompanying digital meters and in temporal graphs. The temporal graphs can be reset individually with the “Reset temp graph” and “Reset current graph” buttons. The button “Temperature read off/on” is very useful if the user is only interested in the temporal trend of the current, since the total sample rate 12-16 Hz then can be used for the current. The current and temperature buttons are used to control the set values of the driver. If the knobs are turned the set value on the driver will immediately change, but if a digital value is written in, the set value will not change until the button “Set digital value” is pushed. With set value we mean the value that the driver wants the laser to achieve. The current changes immediately, but the temperature takes some time to change, since the bulk material has to change temperature as well. "Current limited" indicates the maximum current allowed from the driver. If the current goes over this value the laser turns off automatically. It can be set from the program by writing in a value and clicking on the “Set new current limited” button.

“Power meter” is a program very similar to the control panel. The “Laser type”, “Constant current mode” and “Constant power Mode” indicators are removed and a new temporal graph is introduced as shown in Fig. 4.3.

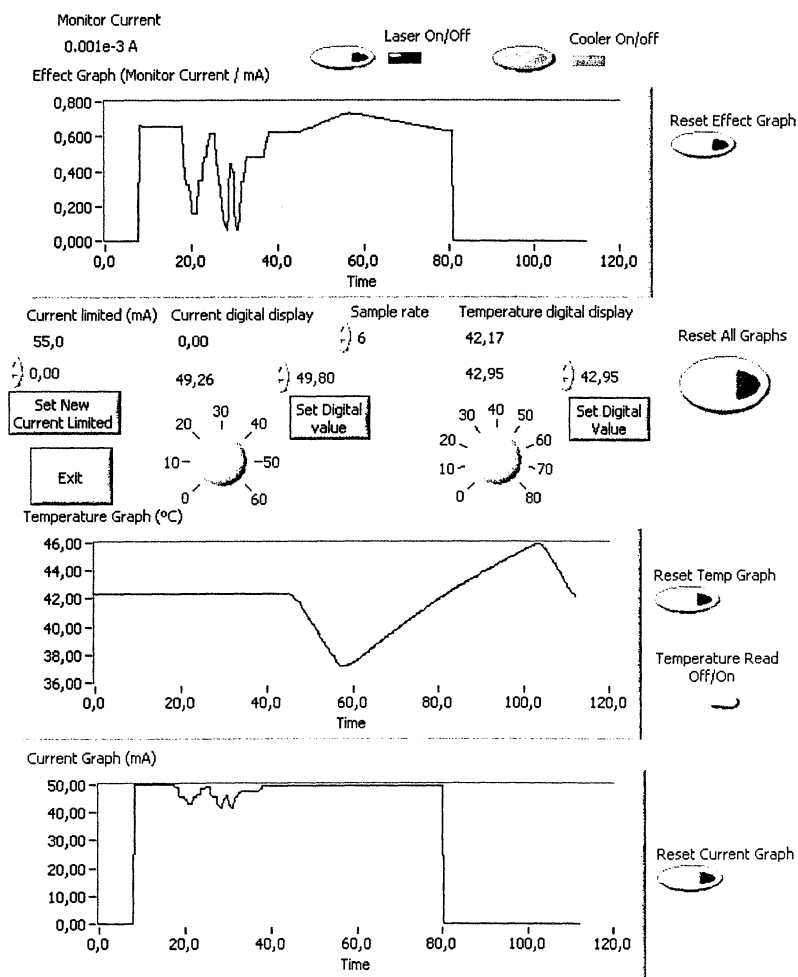


Fig. 4.3 The user interface of the power meter

The new graph is called the "Power graph" and it is showing the monitor current as a function of time. It can be very useful to have a good temporal overview of the three different parameters current, temperature and power at the same time. There is also a new button called "Reset all graphs", that resets all three graphs at the same time, which is good to use if a relation between two or more of the parameters is investigated. The sample rate cannot be set as high as on the "Control panel", since three values are collected from the laser driver each period of time.

"Save driver settings" saves the present settings on the driver to a configuration file. "Load driver settings" loads a saved setting from a configuration file.

## 4.2 Making a diagram over laser power as a function of temperature and current

As described in Chap. 2.1 both the output power and the wavelength of a laser diode depends both on the current and the temperature, but not in the same way. The wavelength gets shorter (more energetic photons) with both higher temperature and current. The power gets higher with higher current, but lower with higher temperature. It is very important to make sure that the maximum recommended output power is not exceeded at any time, in order not to destroy the laser. A diagram over laser power as function of temperature and current makes it easy to see that the values on temperature and current that is going to be used in an experiment do not lead to a power higher than the recommended limit. In Fig. 4.3 the user interface from the "Power 3D graph" program is shown.

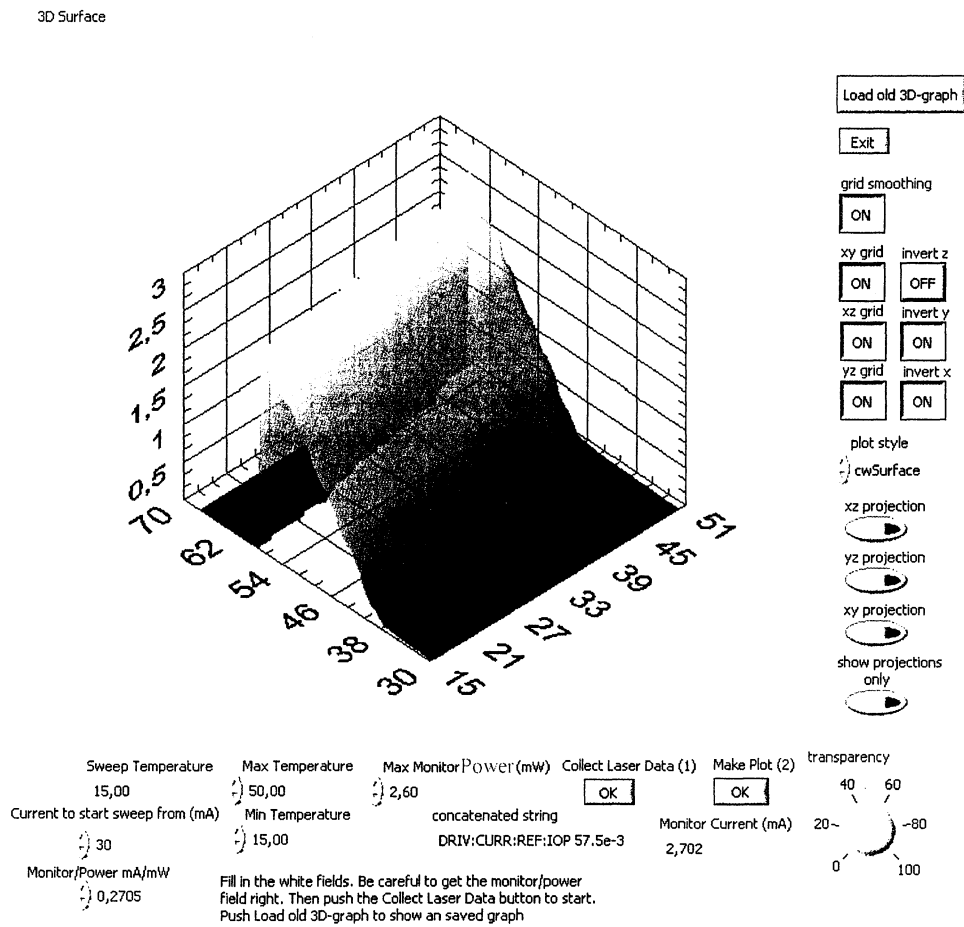


Fig. 4.4 User interface from power 3D graph program

Before this subprogram is used, the user has to make a manual measurement over the monitor current as a function of the output power. This must be done with a regular power meter. It is a linear relationship and changes a little bit for different lasers. When the ratio (monitor current)/(output power) is calculated it should be filled in to the field "Monitor/Power mA/mW". It is very important that this is done correctly, else the laser can be damaged. "Max temperature" and "Min temperature" sets the temperature interval that will be investigated. "Current to start sweep from (mA)" sets the minimum current that will be used. The "Max monitor power (mW)" is the input that indirectly decides the maximum current for each temperature. When the user pushes "Collect laser data" the program will set the laser driver to

the maximum temperature and wait until it stabilizes there. Then the current will be set to "Current to start sweep from (mA)" and the monitor power at that temperature-current pair will be saved. The current then sweeps up in steps of 0.5 mA, measures the power at each step and stops when the measured monitor power is higher than the "Max monitor power (mW)". Then the temperature is decreased one degree and is stabilized there. The current is swept again and this process is repeated until the "Min temperature" has been investigated. In the "Sweep temperature" field it can be seen at what temperature the laser diode is during the measurement. When the measurement is ready and the user pushes the "Make plot" button the 3D graph is shown. All of the buttons on the right side of the screen are different options that affect the appearance of the 3D graph. The "xy-grid", "xz-grid" and "yz-grid" buttons turn the different grids on and off. The invert z, y and x buttons invert the axes. The "Plot style" selector lets the user select different styles to plot the measurement. It can be plotted as a continuous surface or as dots or as contour lines etc. With the projection buttons the projections on different planes can be shown and the "Show projections only" button takes away the graph and shows only the projections. The "Transparency" knob decides how transparent the graph is. It is useful to get a good 3D effect.

### 4.3 Searching for absorption wavelengths

For the subprogram “Searching for absorption wavelengths” to work, more external communication than GPIB is needed. This is accomplished with a PCI-card in the computer called a DAQ (Data AcQuisition). The card used is a National Instruments™, 4472 PCI card. It has eight analog input channels capable of sampling at 102,4 kHz simultaneously. Each channel can handle an input signal of  $\pm 10$  V.

The main purpose of this program is to search for absorption signals when the laser is swept in temperature while the current is kept constant. There is one big advantage with this procedure. If the temperature is stable at 48°C and a GPIB command is sent to put the temperature to 25°C, the temperature adopts every single value between the start and end temperature. There is no physical way for it to jump in discrete steps. So if we can measure the absorption signal fast enough we will be able to see if there are any absorption lines in a wide wavelength range. The DAQ card can measure up to 100 000 samples per second, but it was found to be enough with 1000 samples per second to resolve molecular absorption patterns. In Fig. 4.5 the user interface for the “Searching for absorption wavelengths” program is shown.

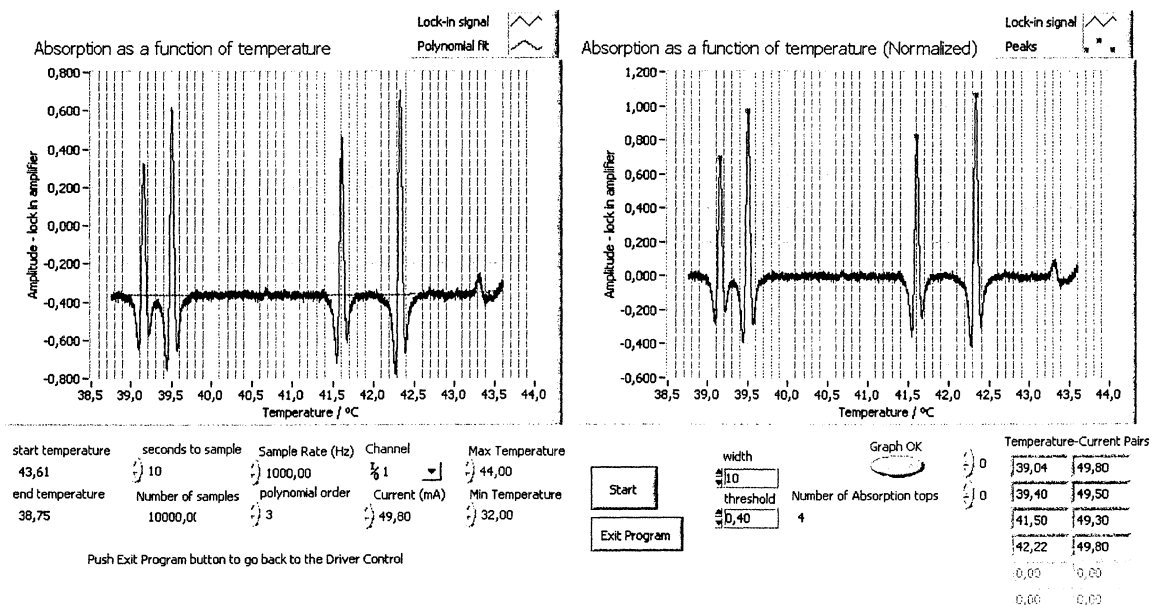
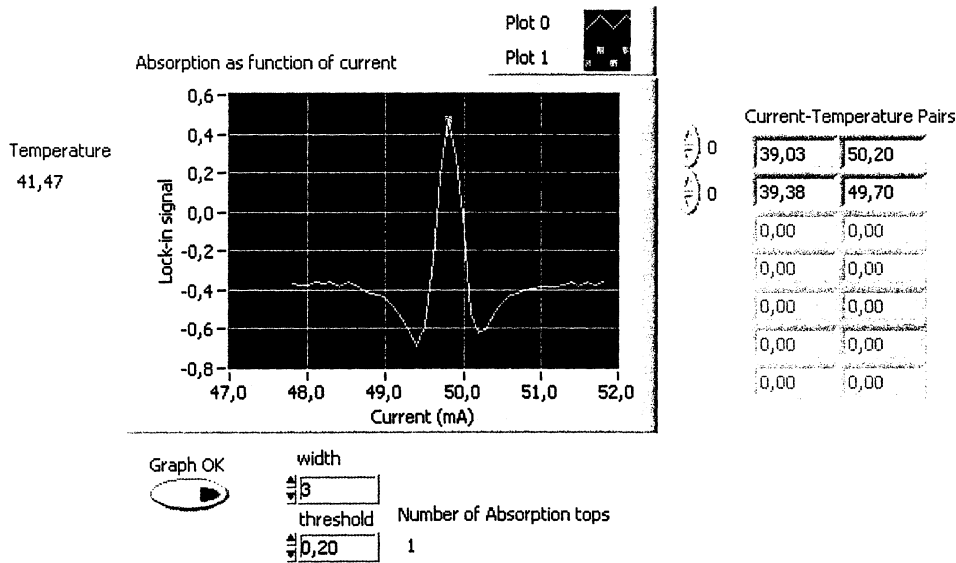


Fig. 4.5 The user interface of the absorption search program

Six parameters under the left windows should be set before the measuring starts. “Max temperature” is the temperature that the driver stabilizes at before it starts the temperature sweep. When it is stable it gets the order to put temperature to “Min temperature”, but “Seconds to sample” is the parameter that decides how long the acquired temperature sweep will be. After this amount of seconds, the sweep is interrupted and the temperature is set back to “Max temperature”. “Sample rate (Hz)” decides at what rate the DAQ card will collect data from the input channels. “Channel” determines which of the DAQ channels that will be used in the measurement. “Current (mA)” is the current that will be used in the measurement. Pushing “Start” will carry out the measurement and plot a graph of the input channel in both the left and right window. The left window is the raw input signal and the red line is a polynomial, of order decided by “Polynomial order”, trying to fit to the baseline of the input signal. “Polynomial order” should be changed until a good fit is reached. In the right window

the plot is moved according to the polynomial so that the baseline lies along zero on the y-axis. In this window, rectangular red dots are placed out by a function that tries to find the peaks of the curve. This function has “width” and “threshold” as input parameters and they should be changed until the correct peaks are marked. Everything under “threshold” will be discriminated by the function and by setting a larger “width” the user can discriminate peaks that are not wide enough, i.e. noise. When the “Number of absorption peaks” indicates the correct number of real relevant absorption peaks in the curve, push “Graph OK”. This starts a subprogram that will investigate each peak individually. The temperature is stabilized at the temperature where the peak was found and then the current is swept around the value used in the absorption search program. Fig. 4.6 shows a picture of this subprogram.



**Fig. 4.6** A picture of the subprogram investigating the absorption peaks with constant temperature while sweeping the current.

The left field “Temperature” is the temperature used at the present measurement. The buttons “Width” and “Threshold” works as in the “Searching for absorption wavelengths” program and when the peak is correctly marked “Graph OK” should be pushed. Then the program stabilizes at the next temperature and sweeps the current. This process is repeated until all of the peaks marked in the “Searching for absorption wavelengths” program are investigated. Then the subprogram closes down and returns the temperature-current pairs to “Searching for absorption wavelengths” program so that the user can see all the peaks in the right graph and have a list of the correct values to use on temperature and current to reach them.

#### 4.4 Multiple DAQ input signals

Since the DAQ card allows 8 input signals at the same time, more sophisticated measurements can be done. This has not been implemented in the package of driver control software yet. But some experiments have been done with this kind of programs.

One interesting aspect is in a project going on right now referred to as time-correlated spectroscopy. In this project it is of great interest to compare different signals with each other in time. This is done with the DAQ card and an example of a recording can be seen in Fig. 4.7.

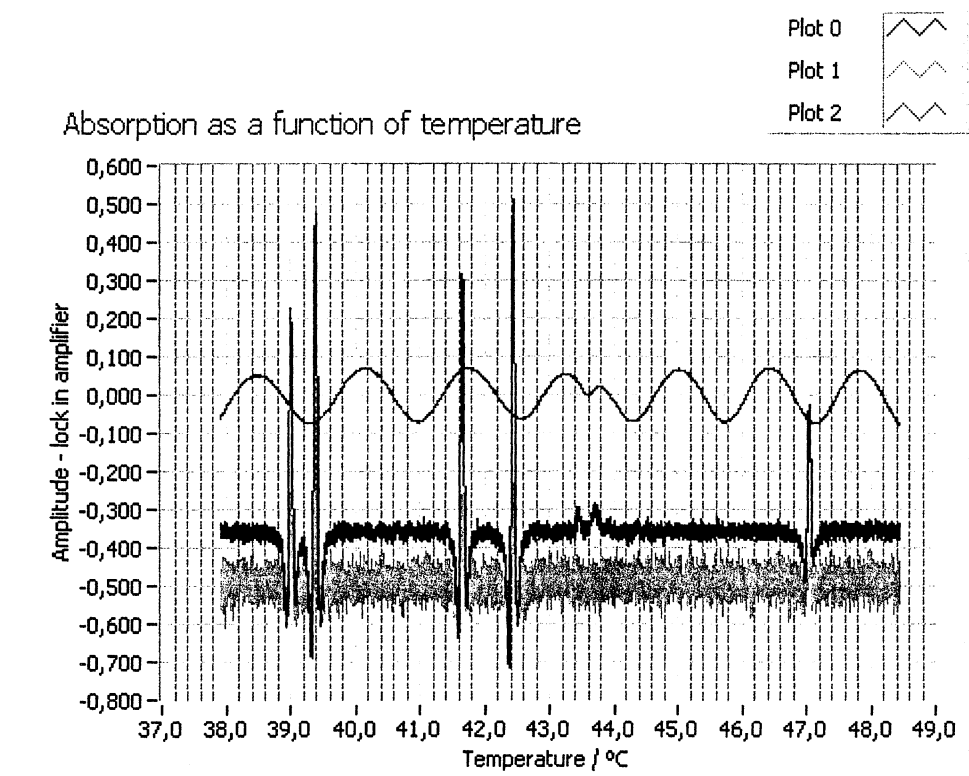


Fig. 4.7 Example of a program measuring multiple signals

The blue signal is in this case a signal from an etalon. When measuring time-correlated spectroscopy and WMS signals it is also interesting to have the direct signals to have something that can normalize the lock-in signal as the power changes with temperature and hence the amplitude of the signals will change as well.

One more thing that is interesting and can be used when measuring multiple channels is that the laser driver has a BNC analog output that can be coupled to a source chosen by the user. One of those sources is the temperature. This means that an analog temperature signal can be sampled with the DAQ card giving an exact temperature scale during the whole measurement. This can be very helpful and will solve the whole problem with the temperature scale, which is more discussed in Chap. 4.5.5.

## **4.5 Implementation of LabView programs**

This chapter describes the implementation of the LabView programs. Some of the basic ideas and the main functions of the different programs will be described. Problems that have been hard to solve will also be mentioned. The solutions to those problems and sometimes solutions that have not yet been implemented will be described as well.

### **4.5.1 Main program – driver control**

Initialization: The program communicates via GPIB with the laser driver and reads in 16 different parameters:

- 1 Factory ID,
- 2 Self test of laser driver,
- 3 Current limit for laser diode,
- 4 Drive mode (constant current / constant power),
- 5 External modulation allowed (on / off),
- 6 Bandwidth,
- 7 Current for laser diode,
- 8 Front output (ground / temperature / current / monitor current),
- 9 Laser type,
- 10 Maximum voltage to thermo electric cooler,
- 11 Maximum current to thermo electric cooler,
- 12 Type of thermal sensor,
- 13 Laser monitor current range,
- 14 Set temperature,
- 15 Photo diode feedback current,
- 16 Thermo electric cooler status.

Those parameters are saved as string variables to be used later for different purposes in the subprograms. Some of them are displayed in the controller display in Fig. 4.1.

Post initialization: The program is waiting for the user to push any of the 7 user buttons on the screen. This is accomplished with a structure that is called event structure in LabView. This structure is programmed to wait for the user to change things on the screen. These user actions are defined by the programmer. When any of the subprogram buttons are pushed, the main program executes it and is put in to a pause mode until the user has exited the subprogram. If the "Exit" button is pushed, the main program is aborted.

### **4.5.2 Save driver settings and load driver settings**

"Save driver settings" reads in all of the 16 settings again as in the main program. Then, it saves it to a user-defined filename with a file structure called configuration data file. This is a platform-independent configuration file where the data is saved in different sections and with separate names on each variable. In Fig. 4.8 a configuration file for the existing GASMAS setup is shown.

"Load driver settings" loads in a configuration file defined by the user. Then all of the variables is sent to the driver so that it gets the same configuration as it had when the configuration file was saved.

```

[Required Commands]
ID="Melles Griot,06DL203A,01307,3.03h"
TST="0,"Self Test OK"
[Current Source Commands]
DRIV_CURR_LIM=" 62.2e-3 A"
DRIV_MODE=0,"curr"
DRIV_MODU_STAT=1,"on"
DRIV_BAND=1,"hi"
DRIV_CURR_REF_IOP=" 57.1e-3 A"
DRIV_OUTP_SEL=0,"Ground"
DRIV_LASE_TYPE=0,"A"
DRIV_CURR_RANG_IMON="0,"0-2 mA"
DRIV_CURR_REF_IMON="0.061e-3 A"
[Thermoelectric Cooler Commands]
TEC_VOLT_RANG=0,"4V"
TEC_CURR_LIM=" 1.2 A"
TEC_SENS_TYPE=0,"AD590"
TEC_TEMP_REF=" 46.00 C"
TEC_STAT=0,"OFF"

```

Fig. 4.8 Configuration file for the existing GASMAS setup

### 4.5.3 Control panel and power meter

Control panel:

Initialization: Six of the parameters read in from the main program are used and displayed by this subprogram as seen in Fig. 4.2. Some of them cannot be used as strings. As all parameters are read in and saved as strings they have to be converted to some kind of variable containing numbers or booleans or extracted to a smaller string. Following variables are used and some of them are converted:

3	Current limit for laser diode	→	double
4	Drive mode	→	boolean
7	Current for laser diode	→	double
9	Laser type	→	string
14	Set temperature	→	double
16	Thermo electric cooler status	→	boolean

Besides those, the laser driver status is read in and converted to a boolean.

Post initialization: There are two loops running parallel.

One of them reads in temperature and current values via GPIB from the laser driver. Here the strings has to be converted to doubles each time the loop is executed. These values are displayed both digitally and on analog meters.

The other loop is an event structure, which was described in 4.5.1. This event structure waits for the user to interact with any of the knobs or buttons on the screen. If the event has to do with the driver, a GPIB command is sent to set the new values. If it is a reset graph command the vector containing the graph is set to zero. If it is "exit" the subprogram is aborted.

It is problematical that the communication speed with the driver is limited by the slow GPIB communication. The subprogram has been implemented so that the user has the ability to turn

off the GPIB command that reads the temperature. This takes away some of the commands in the loop, making it somewhat faster. Besides this there is a setting called "Sample rate" that the user can use to get a faster communication with the driver. "Sample rate" is not the real sample rate, it is the time the loop waits between each execution. This means that if "Sample rate" is set low the waiting time becomes dominating and "Sample rate" is close to the real sample rate but if "Sample rate" is set high the waiting time becomes very small compared to the execution time for the commands in the loop meaning that "Sample rate" is not at all close to the real sample rate.

Power meter:

The "Power meter" is implemented in the same way as the "control panel" with the difference that a third graph has been added. This graph displays the monitor current that is read each time the first loop, the one reading temperature and current values, is executed. The monitor current is proportional to the output power of the laser diode.

#### 4.5.4 Power 3D graph

Initialization: An instruction text, telling the user how to handle the program, is displayed in a box in the user interface and the graph is cleared.

Post initialization: An event structure waits for the user to push any of the buttons: "Collect laser data", "Make plot" or "Load old 3D graph".

If "Load old 3D graph" is pushed, the program loads an old 3D graph that has been saved in three files. One file for the 2D Power matrix and one file each for the current respectively the temperature scale. Then the 3D graph is displayed from a while loop where it is updated for 3D graph settings each time the loop executes.

If "Collect laser data" is pushed, a one-button dialog is shown to the user making clear that the laser will start after the button is pushed. The cooler is turned on, the temperature is set to "Max temperature" and the laser is started with a low current 10 mA, which cannot harm the laser diode. This is a safety precaution, as the temperature may be fluctuating before the experiment starts. Now a subroutine is called. This subroutine checks that the temperature is stable according to a given criteria. The criteria is that 3 temperature readings,  $T_1$ ,  $T_2$  and  $T_3$ , with 2 seconds between them shall be less than 0,4°C away from the wanted temperature and that the differences,  $\Delta T$ , between  $T_1$ ,  $T_2$  and  $T_2$ ,  $T_3$  shall be less than a given number that the programmer defines. This is set to 0,1°C in the "Power 3D graph" program.

Now the measurement starts, GPIB commands are sent to the laser driver and the monitor current is transformed to output power for each measurement. The current is increased stepwise with 0.5 mA until the measured power exceeds the maximum monitor power defined by the user. Then the temperature is decreased with 1°C and the subroutine checking if the temperature is stable is called again. This process continues until the "Min temperature" has been reached and measured on.

If "Make Plot" is pushed the program uses the collected data and makes a 3D graph. The scales are created from the user defined "Max Temperature", "Min temperature" and "Current to start sweep from". The maximum on the current scale in the graph is not defined by the user. It must be changed inside the LabView program. It is predefined to 68 mA. The plot function is inside a while loop that continuous until the user pushes exit. Each time the while loop is executed it is updated with the 3D graph settings from the user interface.

### 4.5.5 Searching for absorption wavelengths

Initialization: An instruction text, telling the user how to handle the program, is displayed in a box in the user interface and the graphs are cleared.

Post initialization: An event structure waits for the user to push any of the buttons: "Start" or "No measurements".

If "Start" is pushed the laser is turned off then the temperature is set to the "Max temperature" and the same stabilization subroutine as described in Chap. 4.5.4 is used to check that the temperature is stable. The same  $\Delta T$ ,  $0.1^\circ\text{C}$ , is used. When the temperature is stable the laser is put on and the temperature is set to the "Min temperature". The program waits 2.5 s before it starts measuring. This is done so that the temperature change will reach its linear part, which is shown experimentally in Chap. 5.3. Just before the temperature sweep is started the current temperature is read, then the measurement starts and the DAQ card collects data for a period of time and a "Sample rate (Hz)" defined by the user.

When the data has been collected, the temperature is read again and then the temperature is set to the "Max Temperature" again. The temperatures read just before and after the measurements are used to create a linear temperature scale. Notice that the "Min temperature" is not supposed to be reached within the time defined by the user. If the temperature gets close to the "Min temperature" while the measurements is going on, the scale will not be linear. The creation of the temperature scale is an empirical formula that might work badly under certain conditions.

When the data has been collected and the temperature scale has been created, a while loop starts that plots two different versions of the same graph. The raw data is interpolated with a polynomial of low order to get a base line of the function. This base line is then subtracted from the raw data, to get rid of most of the unwanted part of the signal, and the result is plotted in the second graph. From this second graph a subroutine tries to find the peaks with a couple of input parameters defined by the user. The while loop continues until the user pushes "graph OK".

When "graph OK" has been pushed a new subprogram starts. This program tries to take care of the problem that the temperature scale is not right and uses the current used in the experiment and the temperatures where the peaks has been found to make a better investigation around each peak. This time the temperature stays stable, this is controlled by the stabilization subroutine mentioned earlier with  $\Delta T = 0.05$ , and the current is swept in 40 discrete steps of 0.1 mA. It starts 2 mA below and finishes 2 mA above the current used in the main program. The DAQ signal is measured for each current. The result is displayed in a graph and the same peak searching subprogram that is used in the main program is used to find the peak. The graph is plotted from a while loop so that the user can change the parameters for the peak function. The loop is executed until the user pushes "graph OK", then next peak from the "Searching for absorption wavelengths" program is investigated.

This process returns a table with temperature-current pair for each peak, which are much better than the initial values from the temperature sweep. There are still problems like hysteresis, which makes the laser diode reach the same wavelength with different values on temperature and current depending on what has happened with the laser diode before, a kind of memory. Another disadvantage is that the subprogram sometimes does not find the peaks because they are out of range of the  $\pm 2$  mA range when the temperature scale is too bad.

Besides this, the temperature-current pairs all have different currents. It would have been better to have a table where all the peaks are listed with temperatures for a specific current. This can be solved with a new better way to measure the temperature scale. The laser driver has an output that can be coupled to the laser diode temperature. This output can be connected to the DAQ card as well. Then we would not be dependent on the slow GPIB communication for any of the measurements. GPIB would only be used to control the laser driver. The method has been tested and it shows good results. The monitor voltage from the temperature has been measured at the same time as the temperature has been read from the laser driver with GPIB. This can be seen in Fig. 4.9. The voltage shows out to be 0.1 V/°C.

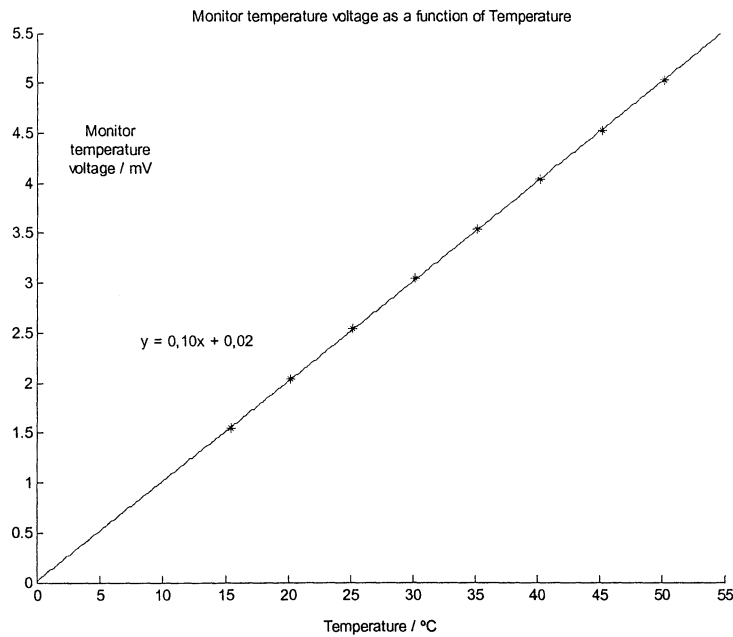


**Fig. 4.9** The monitor temperature voltage as a function of the temperature

The new method to create the temperature scale has not been implemented in this software package yet, but when it is, it will increase the reliability of the measurements.

## 5 Experimental parts

### 5.1 Measurements on Apple

Measurements on apple have been carried out with the equipment described in Chap. 2.4.1 as the existing experimental setup. The GASMAS signal,  $S_{norm}$ , is measured as defined in Eq. 2.5. The absorption wavelength is 761.003 nm and it is an oxygen line in the A band (R7R7). The laser driver is set to 46.0°C and 57.2 mA. An asymmetric saw-tooth signal is superimposed on the driver current with an amplitude of 600 mV and a period of 250 ms. The modulation signal from the function generator is set to 55 kHz and amplitude 200 mV. The metallic laser chamber and the collimator are both flushed with nitrogen to get rid of unwanted oxygen signals. Measurements have been made on different thicknesses of apple with the standard- addition method described in Chap. 2.4.2 and showed in Fig. 2.12. The data is collected, with LabView software via GPIB, from the oscilloscope after averaging 128 times. The apple was cut flat both in top and bottom and the laser light was sent between the center and the edge as showed in Fig. 5.1. The apple used in the study is of Granny Smith type.

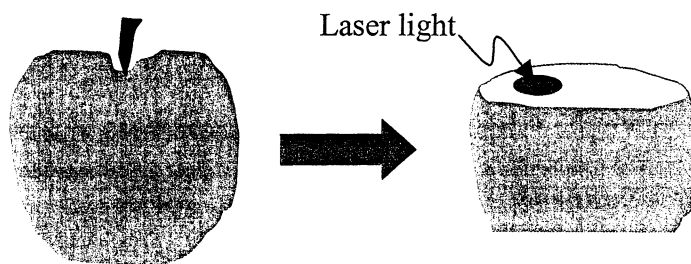


Fig. 5.1 How the apple is cut and the laser light is situated

#### 5.1.1 Apple – thickness 4.0 cm

The first measurement was made with the collimator in direct contact with the apple. Then the collimator was moved away with 0.5 cm at the time. In Fig. 5.2 the GASMAS signal is showed for the case when the collimator is in direct contact with the apple, i.e.  $\Delta x = 0$ . Notice that what is called normalized WMS Signal in this software is a normalized GASMAS signal.

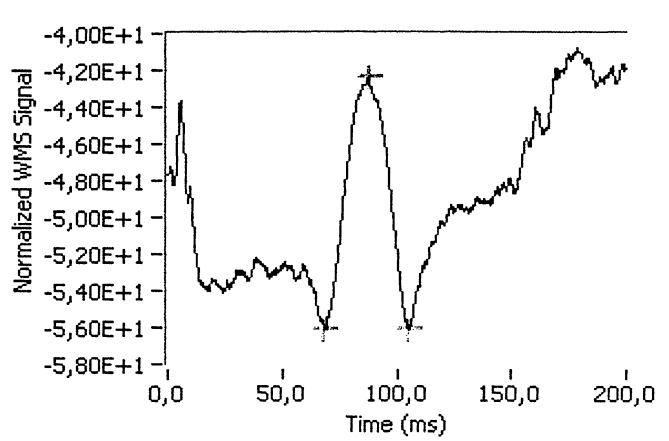


Fig. 5.2 The GASMAS signal for apple 4.03 cm with  $\Delta x = 0$

WMS stands for Wavelength Modulation Spectroscopy and the normalization has been done by dividing with the direct signal shown in Fig. 5.3.

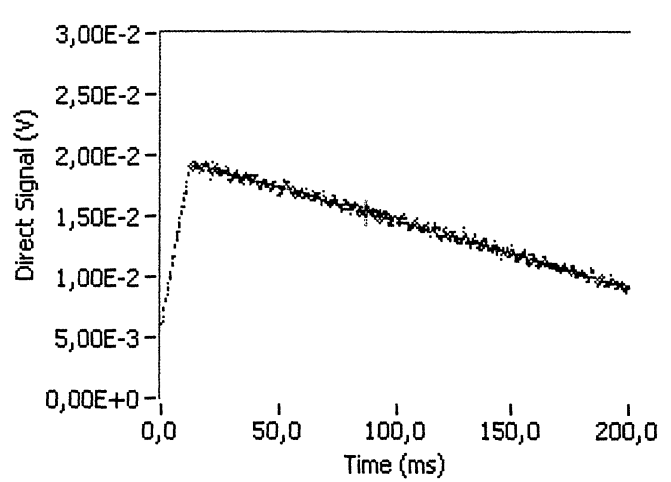


Fig. 5.3 The direct signal for apple 4.0 cm with  $\Delta x = 0$

When the standard addition method was applied, values for  $S_{\text{norm}}$  was achieved for each value of  $\Delta x$ . The values are shown in Table 5.1 and a plot of the values with a fitted straight line is shown in Fig. 5.4.

Added air, $\Delta x$ (cm)	GASMAS signal, $S_{\text{norm}}$
0.0	13.46
0.5	18.26
1.0	20.13
1.5	22.23
2.0	23.05
2.5	24.47
3.0	25.76
3.5	27.15
4.0	28.16

Table 5.1 Values for standard addition method on apple 4.03 cm

In Fig. 5.4 it can be seen that the first value taken at  $\Delta x = 0$  do not resemble good with the other data points.  $L_{\text{eq}}$  is estimated to 4.8 cm, but something seems wrong with the first value. A possible explanation to this phenomenon is that when fruits and vegetables come in contact with air, a diffusion process starts that tries to make the oxygen concentration in the apple pores as large as the oxygen concentration in the surrounding air. It is known that ethylene is produced when vegetables and fruits come in contact with air. Ethylene is important in the process that makes vegetables and fruits ripen, hence it could be interesting if the ethylene concentration could be measured indirectly by measuring on oxygen. A reasonable way to interpret our result is that when the apple is newly cut a fast diffusion mechanism produces a lot of free oxygen in the apple, which affects the ethylene concentration. This process continues but in a much slower rate which does not affect the standard addition method as

much as the earliest value. For this reason a new plot was made not using the first value that is believed to influence with error on the standard addition method.

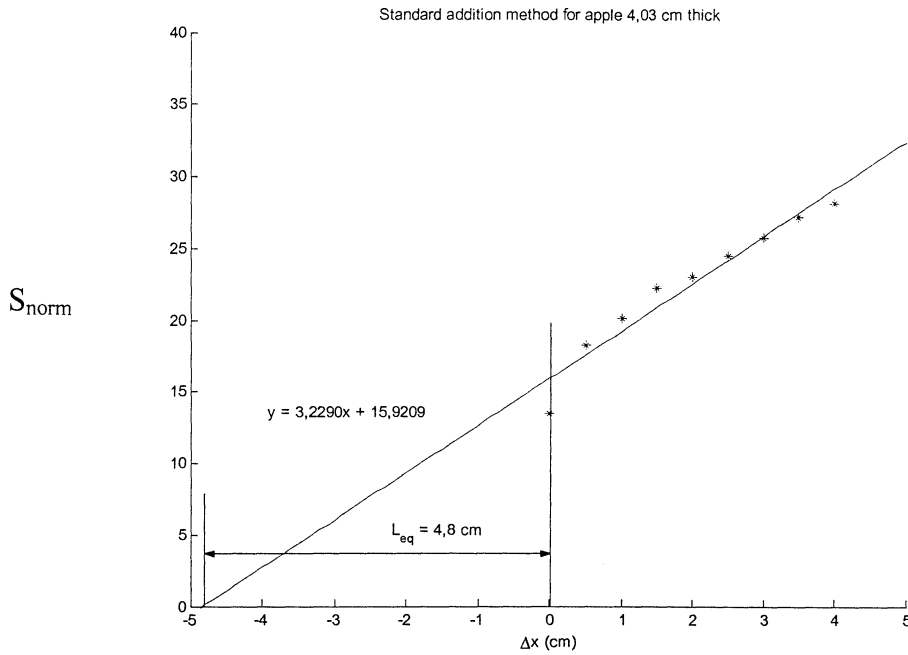


Fig. 5.4 Standard addition plot for apple 4.0 cm

The result of this can be seen in Fig. 5.5.  $L_{\text{eq}}$  is now estimated to 6.3 cm. The most important thing is that the slope of the fitted line has changed from 3.23 to 2.77. As motivated earlier, we have reasons to believe that 2.77 is the better value to use.

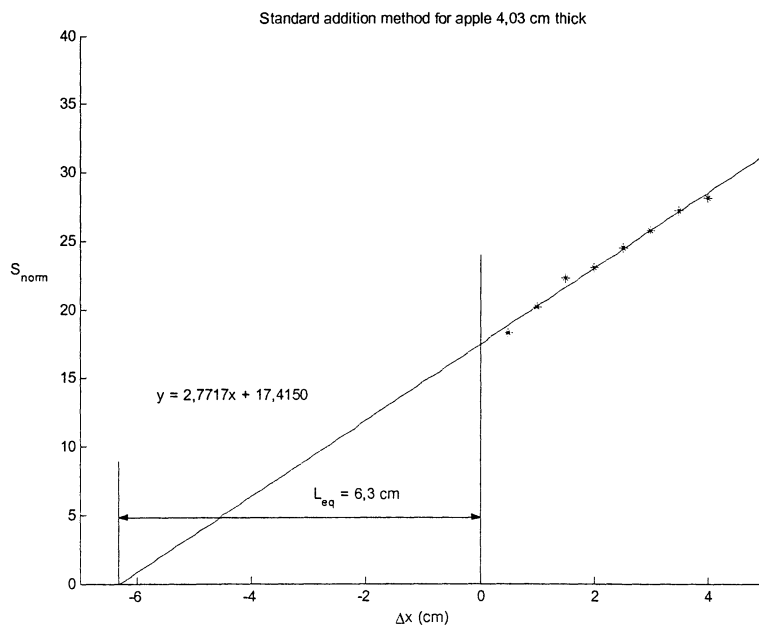


Fig. 5.5 Standard addition plot for apple 4.0 cm with value for  $\Delta x = 0$  removed

### 5.1.2 Apple – thickness 2.0 cm

In this experiment, the same apple as in the former experiment was used. It was divided in two 2.0 cm thick parts. Then the experiment was done in the same way. The collimator was moved in steps of 0.5 cm to carry out the standard addition measurements. The GASMAS signal when  $\Delta x = 0$  is shown in Fig. 5.6.

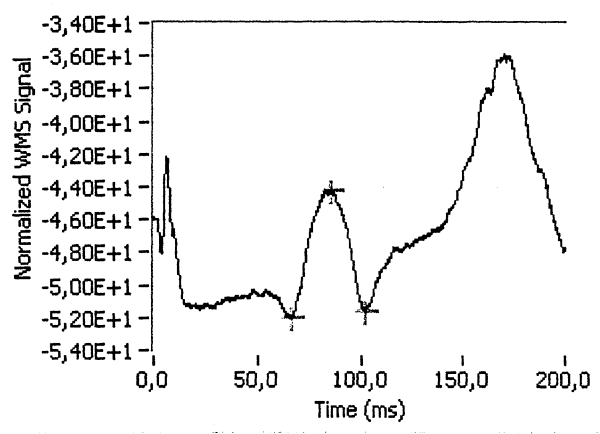


Fig. 5.6 The GASMAS signal for apple 2.0 cm with  $\Delta x = 0$

The direct signal for  $\Delta x = 0$  is shown in Fig. 5.7.

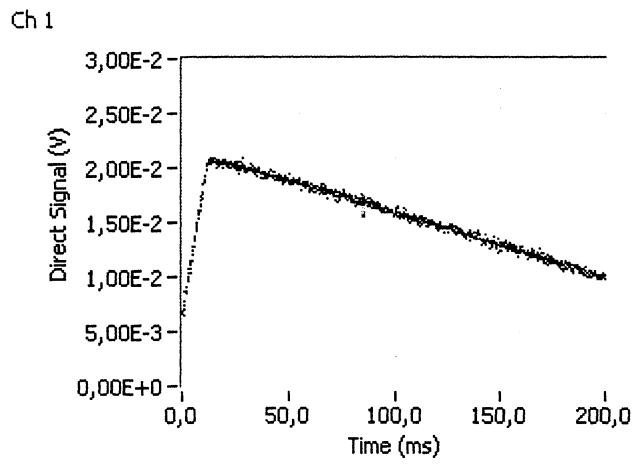


Fig. 5.7 The direct signal for apple 2.0 cm with  $\Delta x = 0$

It can be seen that the GASMAS signal is smaller and the direct signal is greater for the thinner apple sample. This is exactly what we expected as more light is coming through and less oxygen is in the way for a thinner sample. In Table 5.2 the measured value of  $S_{norm}$  is shown. It is interesting to notice that the value of 2 cm added air, 13.44 is very close to the value of the 4.0 cm apple with 0 cm added air, 13.46. This is probably a coincidence, but it means that it does not matter if we let the laser light pass through 2 cm of air or 2 cm of apple.

Added air, $\Delta x$ (cm)	GASMAS signal, $S_{\text{norm}}$
0.0	7.506
0.5	9.700
1.0	11.090
1.5	12.354
2.0	13.438
2.5	14.678
3.0	15.923
3.5	16.988
4.0	18.288

**Table 5.2** Values for standard addition method on apple 2.0 cm

The values are plotted in Fig. 5.8 with a fitted line.

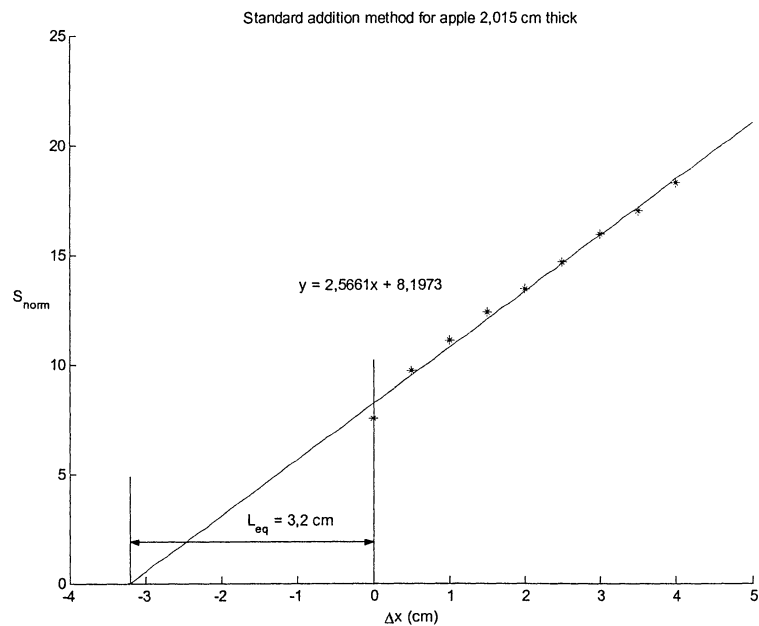


**Fig. 5.8** Standard addition plot for apple 2.0 cm

This time the value at  $\Delta x = 0$  does not resemble as bad as in the previous experiment, but it still deviates from the straight line. This is a little confusing as the apple had been cut much earlier and thus the first value should not have such a divergence from the fitted straight line. It can be interpreted as that the new cut, dividing the apple in two parts, starts a new diffusion process, but not as intensive as the one started in the previous experiment. We tried the same approach as on the thicker piece of apple, made a standard addition plot and fitted a straight line excluding the value at  $\Delta x = 0$ . The result is shown in Fig. 5.9.

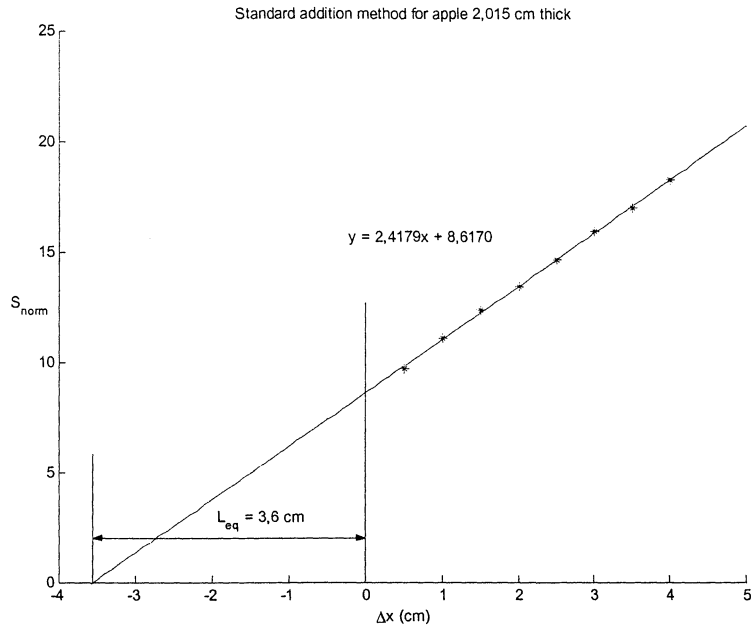


**Fig. 5.9** Standard addition plot for apple 2.0 cm with value for  $\Delta x = 0$  removed

It is obvious that the fit of the straight line is almost perfect, which is a good indicator that the assumption about the diffusion process increasing the oxygen concentration in the apple pores is correct. It seems as though the diffusion process is weaker when the apple is cut the second time, as the fitted line fits very good already when removing the first measurement. Unfortunately there are no time recordings from this experiment, since it was planned only to measure the equivalent path length  $L_{eq}$ , so it is hard to say any thing more substantial about the diffusion process. But diffusion has been investigated on cucumber by the molecular spectroscopy group, Atomic Physics Division, Lund Institute of Technology.

## 5.2 Diffusion measurement on sponge

A sponge contains a lot of air. When it comes in contact with water or some other liquid, it immediately takes up this liquid and rejects some of its air content. Then it is reasonable to believe that the sponge would have a lot of oxygen in gas form inside when it is dry and have less oxygen in gas form inside when it is wet. The problem with this kind of measurement is that both the oxygen gas content and the scattering of the light affect the GASMAS signal. When a wet sponge dries, the gaseous oxygen inside the sponge increases, but at the same time the scattering of the laser light changes inside the sponge as well.

This method is also a way to measure the water content in the sponge without touching it or interfering with it. By sending laser light through the sponge and looking for the inverse of water, which in this case is air containing oxygen, we will be able to decide how damp the sponge is. This could be one way of measuring damp in other contexts as well, e.g. in boards used as building materials.

First a GASMAS signal was measured from a dry sponge. The mean value of  $S_{\text{norm}}$  was in this case 4.43.

Then the sponge was wet down. The measurement was started and the sponge had to dry by itself. The experiment continued almost 14 hours. The same equipments and settings as in Chap. 5.1 were used. 1392 GASMAS signal values,  $S_{\text{norm}}$ , was collected in 13 hours and 46 minutes, which gives 1.7 samples per minute. The result can be seen in Fig. 5.10.

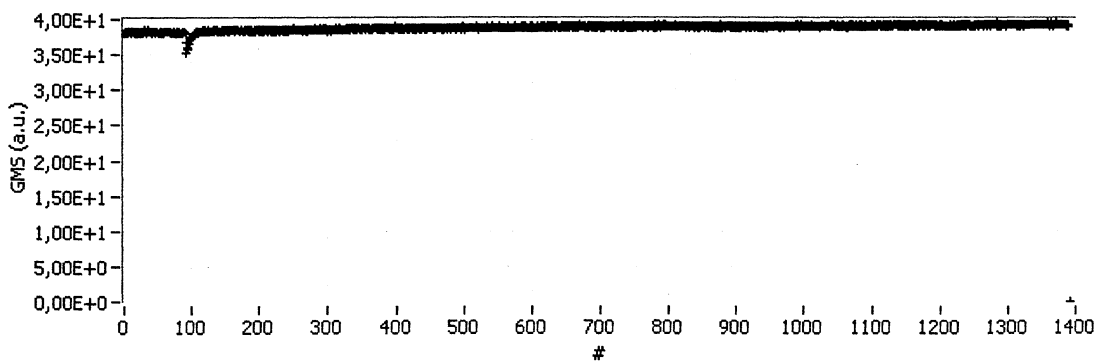


Fig. 5.10 Diffusion measurement on a wet sponge for 13 hours and 46 minutes

Since it is hard to see any details in Fig. 5.10, the important area is zoomed in and showed in Fig 5.11.

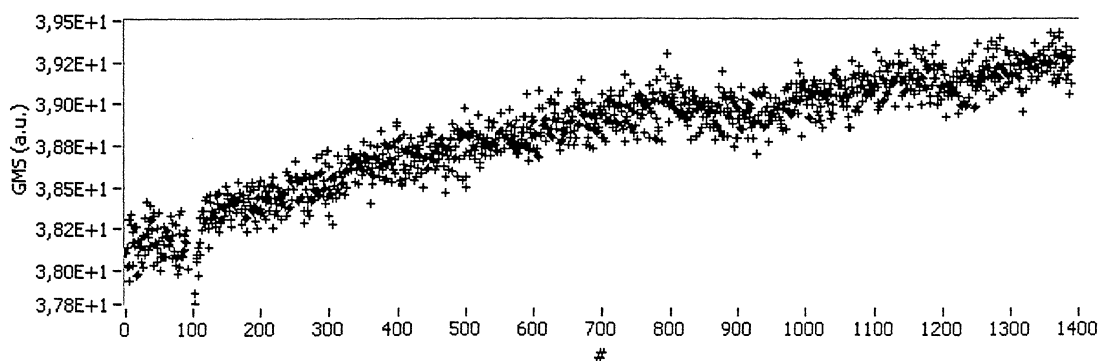


Fig. 5.11 Detail of diffusion measurement on a wet sponge

The GASMAS signal gets stronger as the sponge dries. This is probably due to the increased gaseous oxygen content, but it cannot be taken for sure, as the scattering may affect the signal as well. It will take more experiments with damp to draw any good conclusions. It can be seen that the  $S_{\text{norm}}$  value is around 3.8-3.9 in all of this study. This is far from 4.43 that was measured on the dry sponge. There is uncertainty in this experiment. It was carried out unattended in the lab during the night. This makes it impossible to explain the strange things happening around measurement #100 and measurement #900. To explain or discard those phenomena the experiment has to be made many more times. This experiment was just made to show that the oxygen concentration changes when the sponge dries. This is very reasonable to believe according to the result.

One thing that was surprising was that the sponge was still damp after 14 hours. It was even damp after more than 80 hours. This does not seem to agree with our everyday experience when we put a sponge on the sink. Then it is dry after a couple of hours. But then we wring it out and let it lay free with a lot of air around. In this experiment it was not wrung out and it was put in a small box, 10·10 cm, without any cover and with plastic sheeting in the bottom to let the laser light trough. This box is probably not the best place for any material to get dry.

### 5.3 Measuring the behavior when the temperature is regulated from the laser driver

The laser driver is limiting many of the laser spectroscopy experiments; hence it is important to know how the driver behaves in different situations. We have been measuring the behavior when the temperature has been changed in step sizes from 20.0°C down to 0.01°C. It is interesting to see both how long time the temperature change takes and how the temperature is adjusted around the final temperature by the control circuit. Other interesting aspects are how long the start up time is before anything starts happening with the temperature and if the temperature change is linear when large changes are made.

In Figs. 5.12 – 5.19 the different temperature steps are shown.

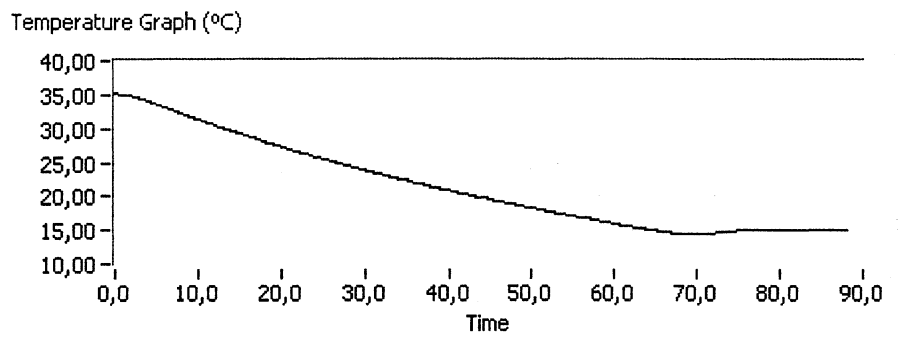


Fig. 5.12 The temperature as a function of time when the temperature change is 20°C

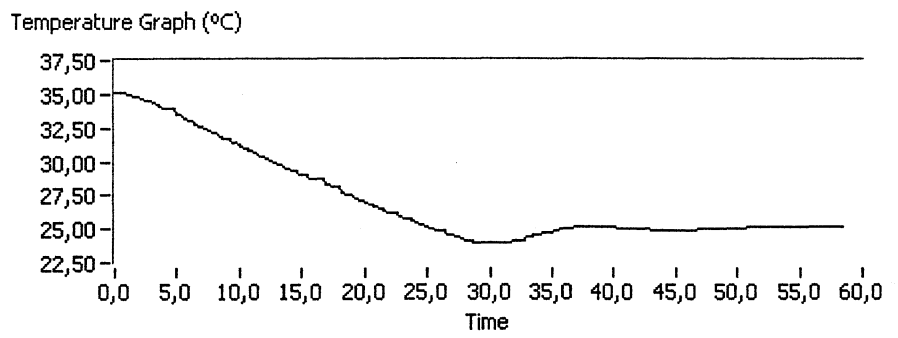


Fig. 5.13 The temperature as a function of time when the temperature change is 10°C

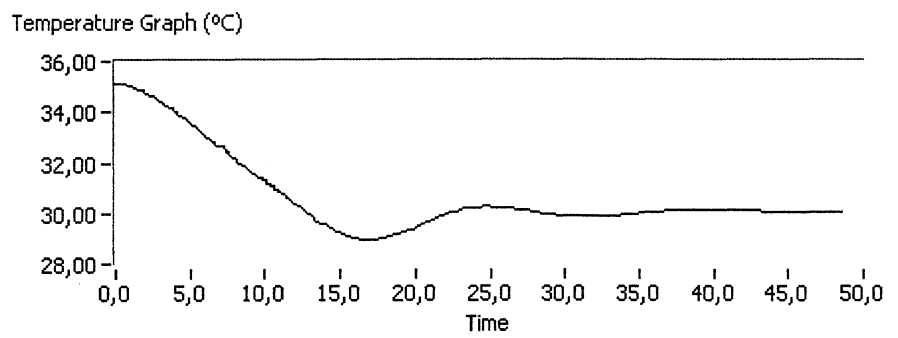


Fig. 5.14 The temperature as a function of time when the temperature change is 5°C

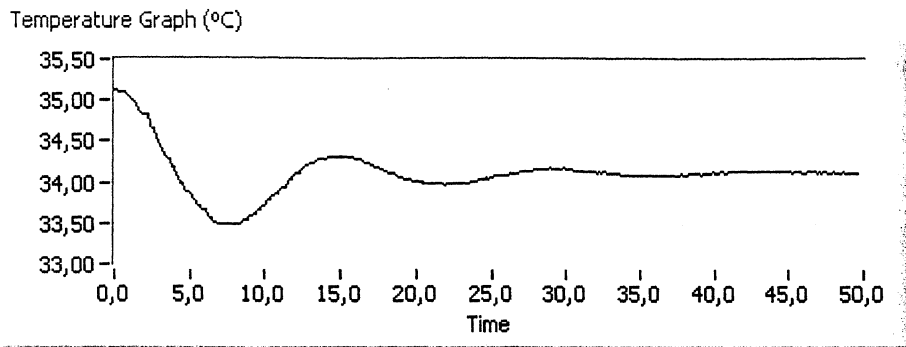


Fig. 5.15 The temperature as a function of time when the temperature change is 1°C

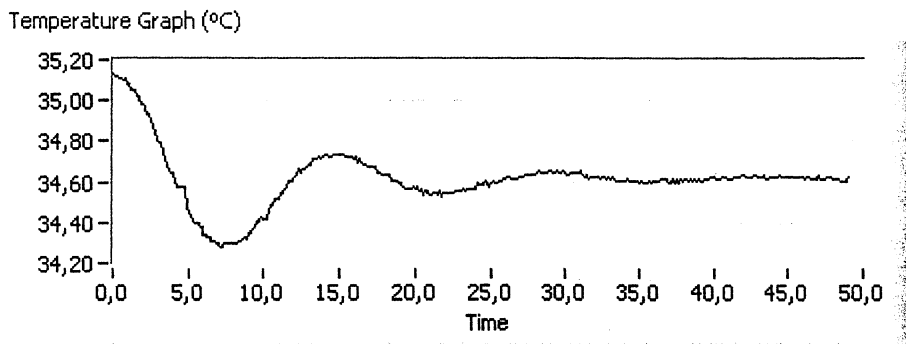


Fig. 5.16 The temperature as a function of time when the temperature change is 0.5°C

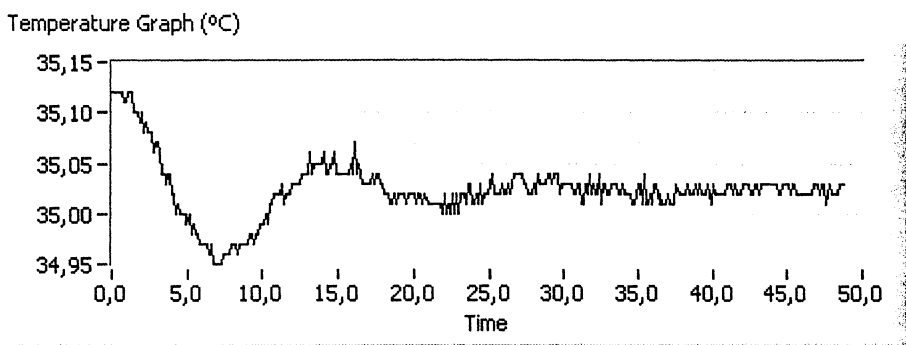


Fig. 5.17 The temperature as a function of time when the temperature change is 0.1°C

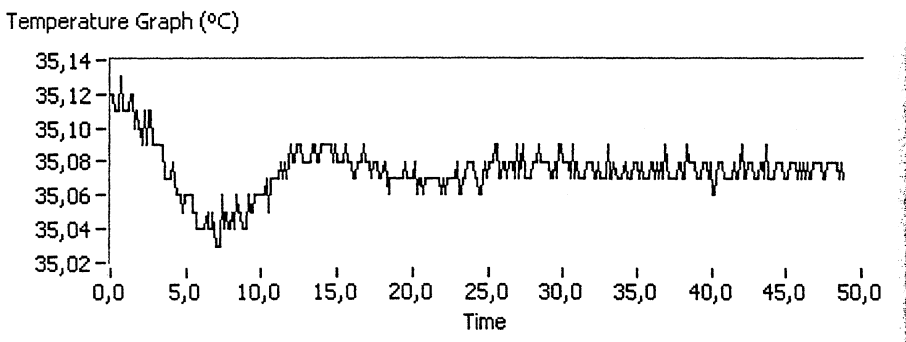
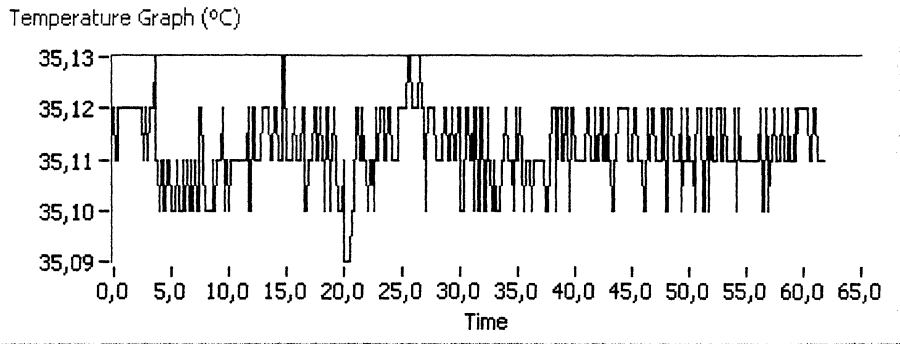


Fig. 5.18 The temperature as a function of time when the temperature change is 0.05°C



**Fig. 5.19** The temperature as a function of time when the temperature change is 0.01°C

The temperature decreases with approximately 0.4 °C/s in the regions that are almost linear. It takes roughly 2.5 seconds for the temperature change to start and become linear. It takes about 50 seconds for the temperature to stabilize when the temperature is changed with 5°C and less. It takes as much as 1 minute and 30 seconds to stabilize on a rough scale when the temperature is changed with 20°C. In Fig. 5.19 it can be seen that when the temperature is changed with 0.01°C it can be hard to notice any difference because the temperature never gets more stable than  $\pm 0.01^\circ\text{C}$ . One thing that is problematical when it comes to fine adjusting the temperature is that the set value on the laser driver has an offset compared to the temperature that is read from the laser diode holder. This means that if the user puts in the value 35.00°C on the laser driver. The laser diode will stabilize at a value around 35.12°C. This can be seen in Figs. 5.12-5-19, where all the temperature decrements has started from 35.00°C set value.

## 5.4 Measuring power as function of temperature and current

These experiments were made with the LabView software that we have developed. The data can be collected and viewed with the software itself, which was shown in Fig. 4.4. But now it was only collected and saved by the software and then we have treated it and made the 3D plots in MATLAB. The first thing that had to be done was to calibrate the power scale. As described earlier in Chap. 4.2 the power is calculated from a monitor current that flows in a photo diode inside the laser holder. These measurements were done on two different laser diodes.

### 5.4.1 Sharp LT030MDO KAI10

The calibration plot is shown in Fig. 5.20. From this it can be seen that the slope of the fitted line is 0.270. The laser has a  $P_{\max}$  of 5 mW and a recommended normal power of 3 mW. We are very careful not to destroy the laser diodes so we try not to exceed 3 mW during our measurements. To be on the safe side a maximum power of 2.6 mW is put in to the software. According to the plot this should be somewhere around 0.7 mA in monitor current.

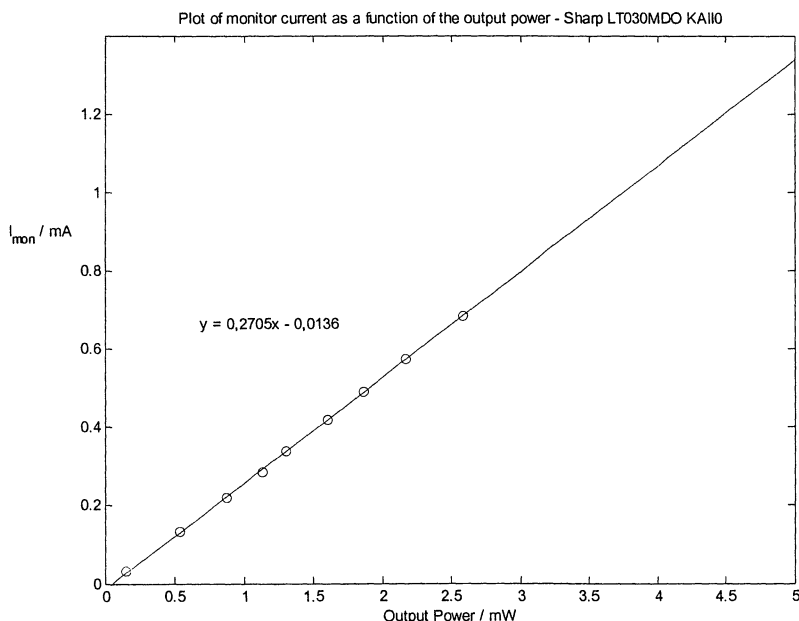


**Fig. 5.20** Monitor current as a function of the output power for Sharp LT030MDO KAI10

The maximum and minimum temperature are 50°C and 15°C respectively. When all parameters were correct in the user interface the program was executed and saved the data for us. The result is shown in Fig. 5.21. This is very useful. Now we now that if we make an experiment and want to use for example the temperature 30°C we should keep the current between 45 and 60 mA. We know both the threshold current to be sure that the laser diode is working as a laser and not as a diode, and the maximum current not to get too high output power at any of the interesting temperatures. When this 3D graph has been made it is easy to go on and use the “Searching for absorption wavelengths” program. Then all the limits can be read from the 3D graph and the laser can be searched through systematically to achieve all possible wavelengths.

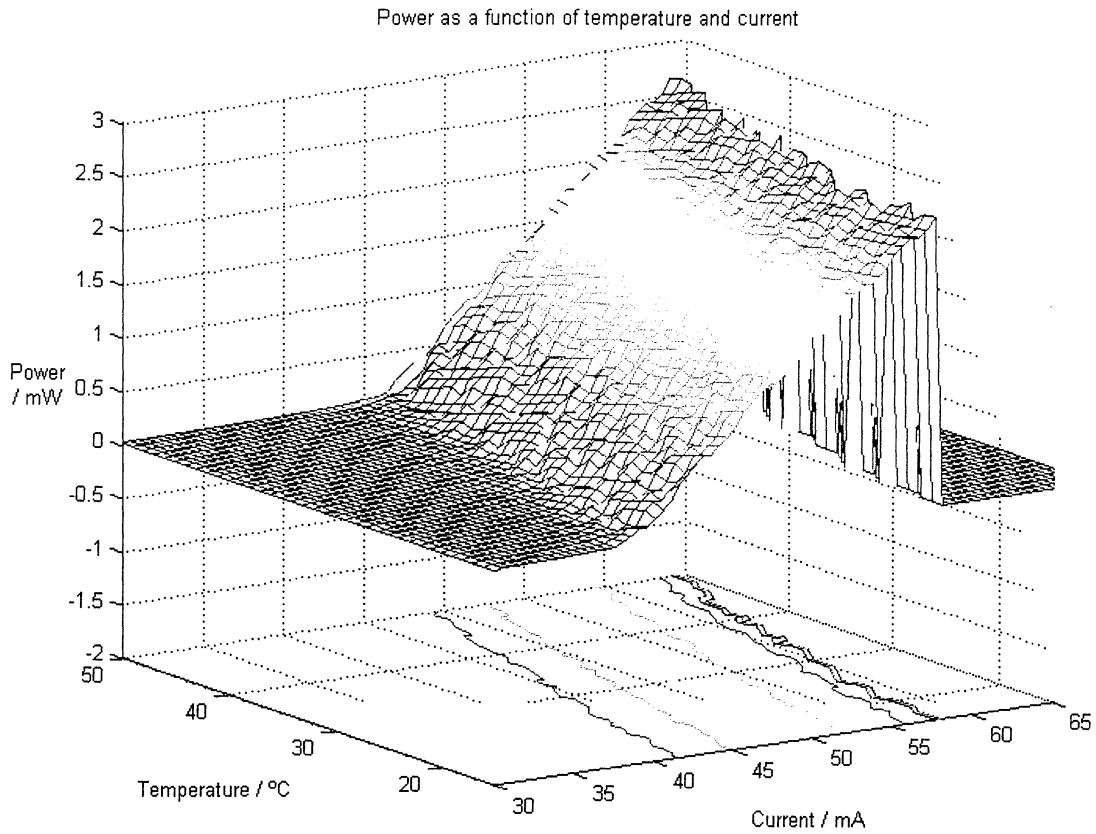


Fig. 5.21 3D graph of power as a function of current and temperature for Sharp LT030MDO KAI10

### 5.4.2 Sharp LT030MDO FA149

The same experiment was made on another laser diode. The calibration plot can be seen in Fig. 5.22.

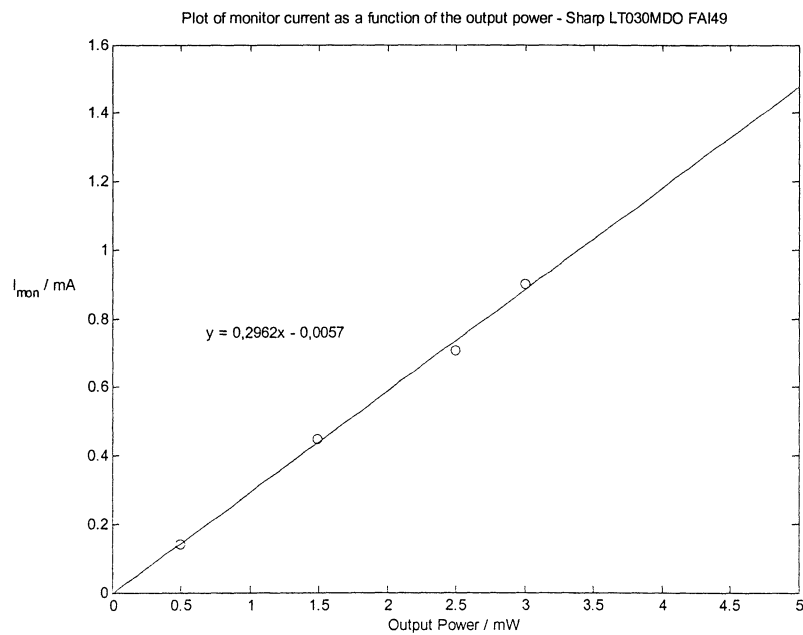
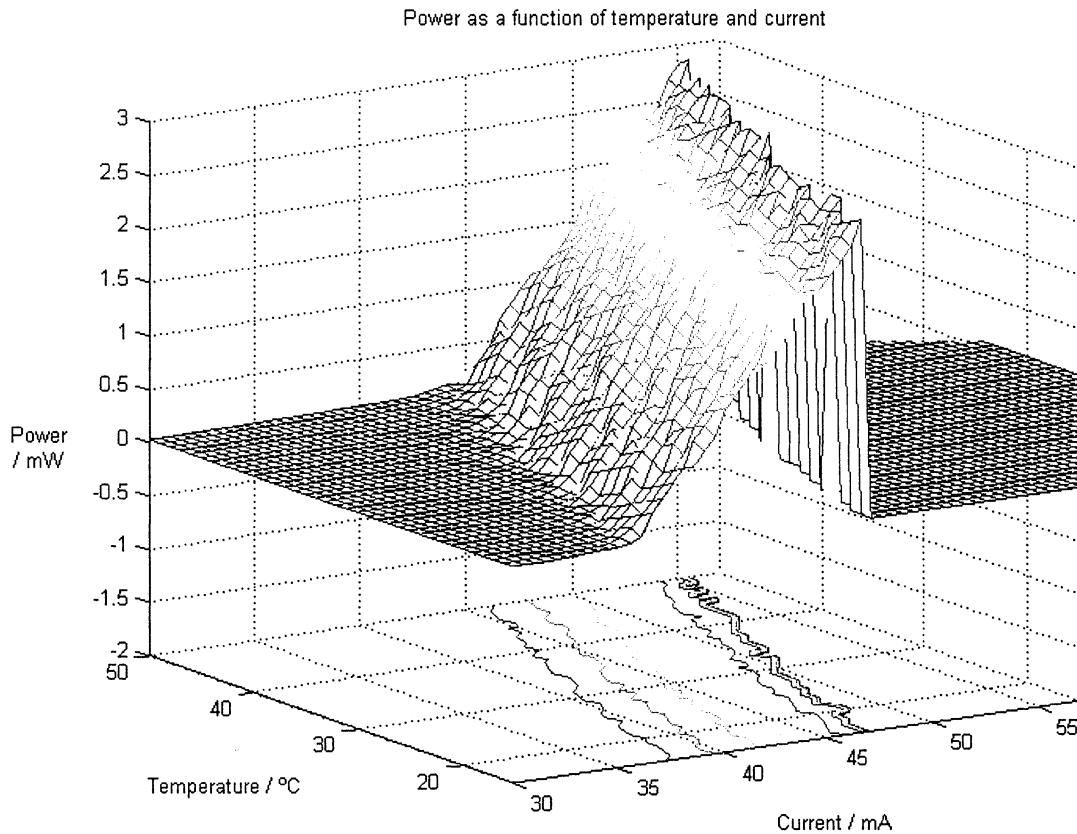


Fig. 5.22 Monitor current as a function of the output power for Sharp LT030MDO KAI10

The slope of the fitted line is 0.296. It is not so far from the value on the other laser, 0.270, which is good because then all laser diodes may be in the same range. This can be useful to have as coarse scale for all lasers making it possible to make quick experiments without having to do calibration plots each time. But as the two laser diodes used in this study were of the same type, it will take experiments with more lasers to be able to draw any conclusions about that. The power 3D graph for this laser diode is shown in Fig. 5.23.



**Fig. 5.23** 3D graph of power as a function of current and temperature for Sharp LT030MDO FAI49

When comparing Figs. 5.21 and 5.23 it is clear that the two laser diodes have totally different  $I_{th}$  and allowed maximum currents. It is interesting to notice that the manufacturer has given the following factory values for the two laser diodes at 25°C.  $I_{th}$  is 34.5 mA for FAI49 and 37.9 mA for KAI10.  $I_{op}$  is 42.7 mA for FAI49 and 49.7 mA for KAI10. This will give an operational power of 1-1.5 mW for both FAI49 and KAI10 according to our measurements.

## 5.5 Searching for absorption wavelengths with the LabView software

These experiments utilize the software that we have been developing within the work of this master's thesis. The subprogram called "Searching for absorption wavelengths" has been used to collect and save the data. The laser diode that has been used is a Sharp LT030MDO 1997FA149 295. It has a nominal wavelength of 756 nm at 25°C and at an operation current of 42.7 mA.

The experiments are made with constant current. Then the temperature is set to the highest value. When the temperature is stable there it is swept down towards a low temperature as fast as the Peltier element in the laser holder can sweep it. This has been made with different temperatures and different currents. The laser light goes through approximately 1 m of air before it hits the laser diode. This means that the absorption, which is due to the oxygen in the air, is large enough to get a good signal. A good signal is wanted in these experiments so that a clear analyze of the different absorption temperatures can be made. Then each peak is investigated closer by having a constant temperature and sweeping the current stepwise over the peak. This procedure produces a table with temperature-current pairs that can be used to reach an absorption wavelength with that particular laser diode. It is important to know the output power at all instances in order not to destroy the laser diode. This has been accomplished by the use of the Power 3D graph software.

### 5.5.1 Current 49.8 mA

A large sweep from 50 to 36 °C shows many of the peaks available at this current. This is shown in Fig. 5.24.

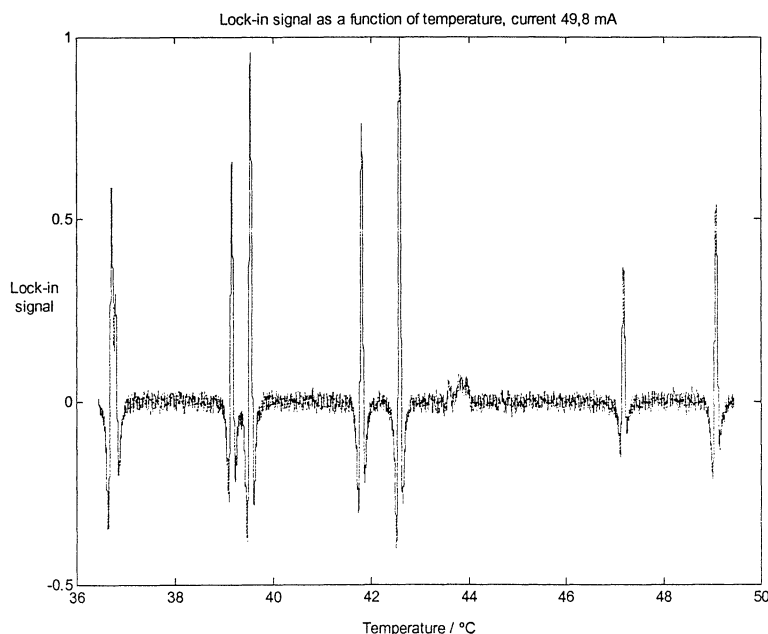


Fig. 5.24 Lock-in signal as a function of temperature at 49.8 mA

In Table 5.3 the temperature current pairs for these peaks are shown. It is clear that the temperature scale in Fig. 5.24 is not really correct. If it had been correct, all the values in the current column should have been 49.8 mA. This problem has been mentioned before and

there is a way to solve it and get better temperature scale but it has not yet been implemented. When this has been implemented the program will be both better due to the new temperature scale and faster when the extra part investigating each peak closer can be omitted. In Table 5.3 there is also a list of which oxygen peaks it is and at which wavelengths those are. This designations are not done automatically. It has been done manually with a wave meter.

Temperature / °C	Current / mA	Oxygen peak	Wavelength / nm
36.669	51.4	-	-
39.063	49.8	R17R17	760.32
39.447	49.0	R15Q16	760.34
41.603	48.5	R15R15	760.46
42.356	48.1	R13Q14	760.51
47.086	48.6	P3Q2	762.79
48.978	49.4	P3P3	762.91

**Table 5.3** Temperature-Current pairs for Fig 5.24

Other sweeps at this current where made as well. No one of them gave any new information. One of them showing a little smaller range of the temperature span is shown in Fig 5.25. An interesting thing is the small saw-tooth formed peak between 43 and 44 °C. This has been investigated closer and was found to be a mode jump. That investigation was made with a spectrometer that gave us the possibility to see if the laser was running in single mode or multi mode and if any sudden jumps in wavelength occurred. At this spot around 43.3°C the laser went into multi-mode behavior and jumped a bit in wavelength. This is typical for mode jumps. At all other instances the laser seems to be running single mode.

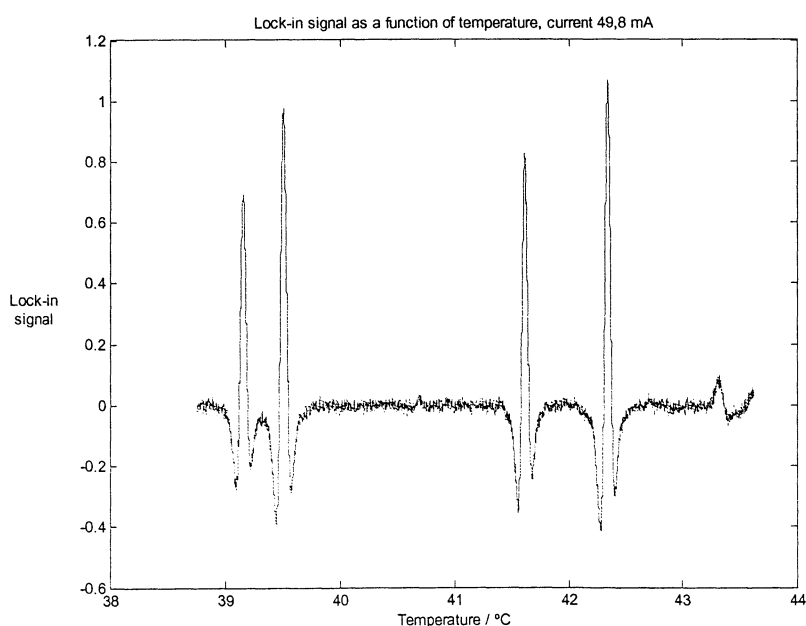


**Fig. 5.25** Lock-in signal as a function of temperature at 49.8 mA

### 5.5.2 Current 47.0 mA

At this current two of the sweeps that were made show the characteristics of the laser diode. Fig. 5.26 shows the higher temperatures and Fig. 5.27 shows the lower temperatures.

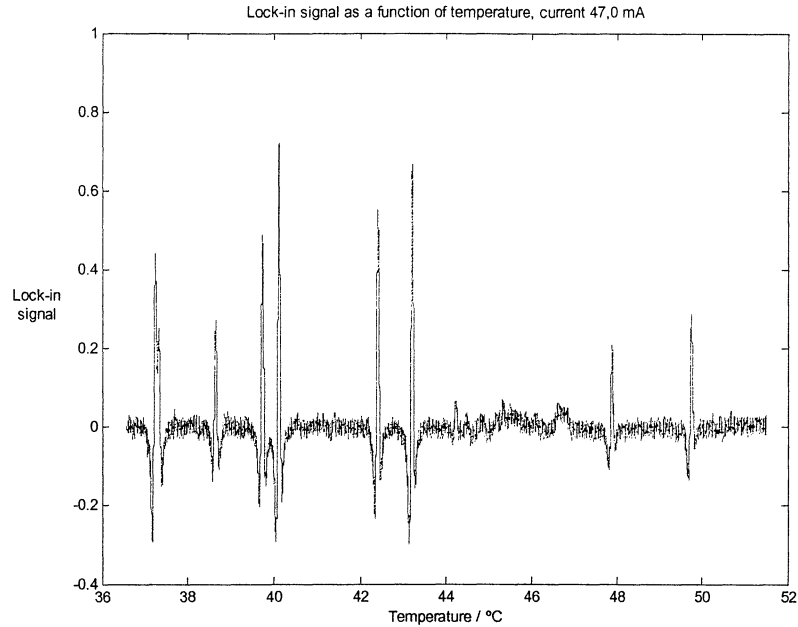


Fig. 5.26 Lock-in signal as a function of temperature at 47.0 mA

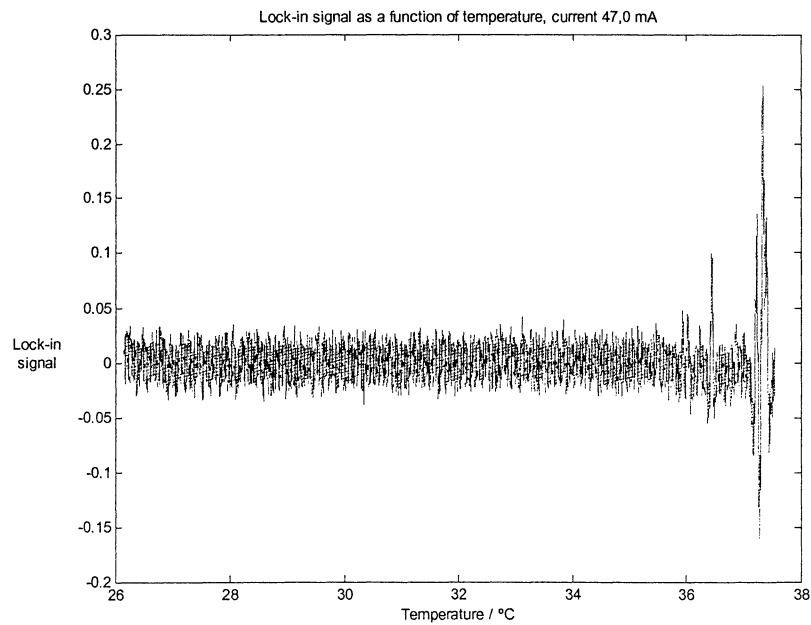


Fig. 5.27 Lock-in signal as a function of lower temperature at 47.0 mA

At the lower temperatures there are no absorption at all. This means that all interesting information is shown in Fig. 5.26. In Table 5.4 the temperature-current pairs for Fig. 5.26 is shown. On some of the temperatures the current is omitted. This has to do with the problem

with the temperature scale. The program has failed to find the peaks by itself. With the better temperature handling that will be implemented this problem will not occur.

Temperature / °C	Current / mA
37.144	48.2
38.536	47.0
39.622	45.9
40.008	45.5
42.309	-
43.099	-
47.769	-
49.646	45.7

**Table 5.4** Temperature-Current pairs for Fig. 5.26

One area just beneath 37.5°C looks different from the rest of the peaks. The temperature was swept over this area again to make sure that the appearance was not accidental. The result is shown in Fig. 5.28. Unfortunately there was no possibility to check this area with the spectrometer. Then it could have been decided if these peaks are mode jumps or absorption peaks.

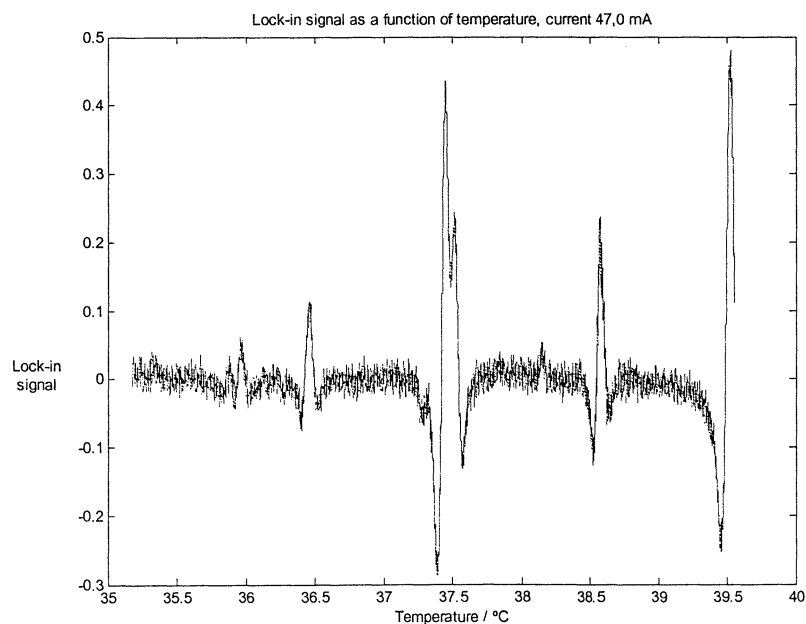


**Fig. 5.28** Close up of lock-in signal as a function of temperature at 47.0 mA

It can also be seen from Fig. 5.26 and Fig. 5.28 that the peaks are not situated at the same temperatures. This has to do with the uncertainty in the temperature scale.

### 5.5.3 Current 45.0 mA

The measurement at 45.0 mA showed that the absorption patterns do not look the same at different currents. The air has not changed, thus the behavior of the laser is different at different currents, which is just what we had expected. In Fig. 5.29 it is shown that some of the peaks at the higher temperatures can no longer be seen and to the left of the double peaks at 40°C a strange pattern shows. There is a big probability that the strange pattern is a mode jump but it has not been investigated yet.

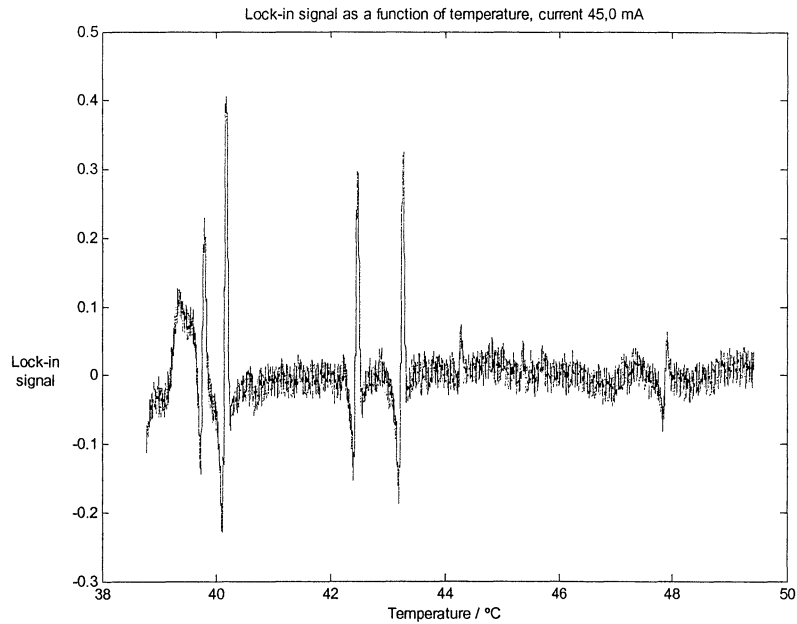


**Fig. 5.29** Lock-in signal as a function of temperature at 45.0 mA

At this moment, without further research there is not much more to say about Fig. 5.29. The temperature-current pairs are shown in Table 5.5.

Temperature / °C	Current / mA
39.699	45.5
40.078	45.4
42.366	44.4
43.153	-

**Table 5.5** Temperature-Current pairs for Fig. 5.29

## 6. Conclusions and summary

The GASMAS method has been investigated and the existing GASMAS equipment has been used and verified to work as described in earlier papers [2.11, 2.13].

Research about the Stark effect has been carried out to find out if there can be any possibilities to measure electric fields inside a bulk material with the GASMAS method. In [3.3] measurements on electric fields in free air has been done. With this knowledge and theory from [3.4] it seems as it would be possible to do this kind of measurements using  $\text{NH}_3$  as the electric field sensitive gas at  $1.23 \mu\text{m}$ . If the electric field is well known the method might be used to get information about the gas distribution using tomography.

A software package for controlling the laser diode driver and handling analogue input signals has been implemented using LabView. It consists of a main program called the laser driver control. From this main program it is possible to reach the different subprograms: Control Panel, Power Meter, Power 3D graph and Search for absorption. Control Panel and Power Meter are used to control the basic settings on the driver and to have a graphical overview over the settings and the temporal evolution of the current, temperature and power of the laser diode. Power 3D graph makes a plot of the output power as a function of temperature and current, which is very useful to have to make sure that the maximum power is never exceeded at any time during experiments, e.g. during GASMAS experiments when the current is swept over wide areas. Search for absorption is used to search through the entire wavelength span of a laser diode to see where the light is absorbed by the gas it passes on the way to the detector. This is useful for the characterization of new laser diodes and to see if they are possible to use in absorption measurements, e.g. in GASMAS.

Experiments have been made to verify the GASMAS method and the functionality of the software package. The equivalent path length,  $L_{\text{eq}}$ , has been calculated for two apple pieces with different thicknesses. Diffusion measurement has been made on a sponge. A wet sponge was drying by itself for 14 hours. The normalized GASMAS signal got stronger during this period of time. This can have two reasons. One of them, more air inside the sponge, is predicted to give stronger signal. More air and hence more gaseous oxygen got into the sponge when it dried. The other reason is that the scattering properties of the material changes as the sponge dries. It is harder to say how this affects the signal. It cannot be evaluated from this measurement, but a time-resolved measurement would shed light on this.

The behavior of the temperature for different changes in temperature, from  $0.01^\circ\text{C}$  to  $20.0^\circ\text{C}$ , has been studied. It was calculated that the temperature changes with about  $0.4^\circ\text{C/s}$  while it is in the linear part of a temperature excursion. It could be seen that 50 s is a minimum time to wait for the laser diode to stabilize on a new temperature if it is changed with  $5^\circ\text{C}$  or less.

Two different laser diodes have been characterized with output power as a function of temperature and current.

One laser diode has been searched over the whole wavelength span to detect oxygen absorption. One definitive mode jump was found and other differences at different temperatures were found as well. Eight oxygen absorption peaks were found and six of them were characterized with wavelength and spectroscopic designation.

## 7. Future Work

The Stark effect project has only started. There is a great challenge in making practical experiments. A usable gas cell with electrodes has to be built. Then a laser matching the  $\text{NH}_3$  wavelength,  $1.23 \mu\text{m}$ , has to be found and bought. Furthermore, a high voltage source that can be modulated by an external function generator would be very useful when it comes to doing sensitive lock-in measurements.

The basic software package is finished. Some new features may be implemented. The construction of the temperature scale in the find absorption wavelength program should be redone as described in Chap. 4.5.5.

This software package has to be integrated and completed with GASMAS measurement applications. Then the natural way of doing GASMAS measurements would be an automatized process. The 3D power graph program transfers information to the search for absorption program, which automatically searches for absorption peaks in the lasers wavelength range. Maybe the program can be equipped with a part that recognizes the spectrum and identifies the absorption peaks as well. Then the user can choose which peak/peaks to use for GASMAS measurements. This should be done from a user-friendly interface that lets the user decide if diffusion measurements, standard addition measurements or individual GASMAS measurements should be performed. If a portable handheld GASMAS equipment shall be developed, the DAQ card will preferable be used as a lock-in amplifier as well. This will need a lot of complicated LabView programming.

As mentioned in Chap. 5.2 diffusion measurements on drying objects has to be investigated closer. It is hard to tell how the scattering and oxygen influences the GASMAS signal individually. If time resolved measurements are done at the same time as the GASMAS signal is acquired, it can be determined if the scattering changes. Henrik Fält in the Molecular Spectroscopy Group, Atomic Physics Division, Lund Institute of Technology is directing his Master's thesis towards the phase shift method, which will give us the opportunity to do time resolved measurements with the normal GASMAS equipment.

## 8. Acknowledgements

I would like to thank my supervisor *Sune Svanberg* for his help and all his enthusiastic ideas about what GASMAS can be used for. He has also helped me a lot by reading through the manuscript numerous times. I appreciate his way of making physics easier to understand.

Without *Mikael Sjöholm* the experimental parts of this thesis would have taken much more time. He has also introduced LabView to me and helped me out when I got stuck with some technical LabView details. He has made a great job reading through the manuscript of this thesis and been helpful when I have needed to discuss atomic physics theory. Thank you for all your help!

I would also like to thank *Linda Persson* who welcomed me and helped me with everything when I started my project this summer when most of the people in Atomic Physics Division were out of office. She has also helped me put boundaries to my work and made sure that I got my experiments done.

The expert on the practical diode laser physics in our group, *Gabriel Somesfalean*, has helped out despite his lack of time, as he is starting to come close to his dissertation. I would like to thank him for sharing his experience of laser diode physics and what it means to be working at the Atomic Physics Division.

I would like to thank our Chinese friend *Gao Hong*. She has helped me a lot with my experiments and been around in the lab, also teaching me some chinese! She also helped me by identifying the oxygen peaks in Chap. 5.5.1

Of course, I would also like to thank *Rasmus Grönlund* and *Henrik Fält* for being around supporting me if needed. *Magnus Bengtsson* has been a real great person to talk to about everything and he has made me feel welcome at the department.

A big thank to all my friends during the education, you know who you are.

Finally, I would like to thank my girlfriend *Sofie* and my family for always supporting me with everything I need to survive. Without them it would have been hard to finish this. Thank you!

## References

- 2.1 R. N. Hall, G. E. Fenner, J. D. Kingsley, T. J. Soltys, and R. O. Carlson, *Coherent light emission from a GaAs junction*, Phys. Rev. Lett. **9**, 366 (1962)
- 2.2 M. I. Nathan, W. P. Dumke, G. Burns, F. H. Dill, Jr., and G. Lasher, *Stimulated emission of radiation from GaAs p-n junctions*, Appl. Phys. Lett. **1**, 62 (1962)
- 2.3 N. Holonyak, Jr. and S. F. Bevacqua, *Coherent (visible) light emission from Ga(As<sub>1-x</sub>P<sub>x</sub>) junctions*, Appl. Phys. Lett. **1**, 82 (1962)
- 2.4 T. M. Quist, R. H. Rediker, R. J. Keyes, W. E. Krag, B. Lax, A. L. McWhorter, and H. J. Zeigler, *Semiconductor maser of GaAs*, Appl. Phys. Lett. **1**, 91 (1962)
- 2.5 U. Gustafsson, *PhD Thesis, Diode laser spectroscopy in extended wavelength ranges* (Lund Institute of Technology, Lund 2000)
- 2.6 O. Svelto, *Principles of Lasers*, 4<sup>th</sup> ed. (Plenum Press, New York 1998)
- 2.7 S. M. Sze, *Semiconductor devices, physics and technology*, 2<sup>nd</sup> ed. (John Wiley & Sons, New York 2002)
- 2.8 J. M. Supplee, E. A. Whittaker, and W. Lenth, *Theoretical description of frequency modulation and wavelength modulation spectroscopy*, Appl. Opt. **33**, 27 (1994)
- 2.9 S. Svanberg, *Atomic and molecular spectroscopy: basic aspects and practical applications*, 3<sup>rd</sup> ed. (Springer-Verlag, Berlin, Heidelberg 2001)
- 2.10 J. H. Scofield, *A frequency-domain description of a lock-in amplifier*, Am. J. Phys. **62**, 129 (1994)
- 2.11 M. Sjöholm, G. Somesfalean, J. Alnis, S. Andersson-Engels, and S. Svanberg, *Analysis of gas dispersed in scattering media*, Opt. Lett. **26**, 16 (2001)
- 2.12 M. Sjöholm, *Master's Thesis, Development of a laser spectroscopic technique for gas in scattering media* (Lund Institute of Technology, Lund 2001)
- 2.13 G. Somesfalean, M. Sjöholm, J. Alnis, C. Af Klinteberg, S. Andersson-Engels, and S. Svanberg, *Concentration measurement of gas embedded in scattering media by employing absorption and time-resolved laser spectroscopy*, Appl. Opt. **41**, 18 (2002)
- 2.14 S. Andersson-Engels, R. Berg, S. Svanberg, and O. Jarlman, *Time-resolved transillumination for medical diagnostics*, Opt. Lett. **15**, 1179 (1990)
- 3.1 S. Höjer, and H. Ahlberg, *Spatially resolved measurements of electric field distributions in gas-insulated high voltage components using a CO<sub>2</sub> laser probe beam*, Appl. Opt. **27**, 18 (1988)

- 3.2 G. Herzberg, *Molecular spectra and molecular structure - spectra of diatomic molecules*, 2<sup>nd</sup> ed. (Van Nostrand, New York 1950)
- 3.3 S. Höjer, *Infrared laser spectroscopic methods for temperature and electric field strength measurements*, Technical Report No. 200 (Chalmers University of Technology, Göteborg 1990)
- 3.4 H. Sasada, *Stark-modulation spectroscopy of NH<sub>3</sub> with a 1.23- $\mu$ m semiconductor laser*, Opt. Lett. **9**, 448 (1984)